

APPLICATION OF COSMIC-RAY SHOCK THEORIES TO THE CYGNUS LOOP: AN ALTERNATIVE MODEL

AHMED BOULARES AND DONALD P. COX
 Physics Department, University of Wisconsin, Madison
 Received 1987 October 30; accepted 1988 March 25

ABSTRACT

Steady state cosmic-ray shock models are investigated in light of observations of the Cygnus Loop supernova remnant. In this work we find that the model of Völk, Drury, and McKenzie, in which the plasma waves are generated by the streaming instability of the cosmic rays and are dissipated into the gas, can be made consistent with some observed characteristics of Cygnus Loop shocks. The waves heat the gas substantially in the cosmic-ray precursor, in addition to the usual heating in the (possibly weak) gas shock. The model is used to deduce upstream densities and shock velocities using known quantities for Cygnus Loop shocks. Compared to the usual pure gas shock interpretation, it is found that lower densities and approximately 3 times higher velocities are required. If the cosmic-ray models are valid, this could significantly alter our understanding of the Cygnus Loop's distance and age and of the energy released during the initial explosion.

Subject headings: cosmic rays: general — nebulae: individual (Cygnus Loop) — nebulae: supernova remnants — shock waves

I. INTRODUCTION

Observations of shock waves driven by supernova remnants (SNRs) have been interpreted almost exclusively (and fairly successfully) as though the shocks were ordinary hydrodynamic discontinuities. In such models, the inflowing gas is slowed and compressed by the shock; the converted kinetic energy is thermalized in the gas (e.g., Courant and Friedrichs 1948; Zel'dovich and Raizer 1967). If radiation by the heated gas is rapid, the shock structure also includes cooling and recombination regions following the initial jump (e.g., Cox 1972; Raymond 1979; Raymond *et al.* 1983). Evidence that supports such a view includes UV and X-ray observations of hot highly ionized gas just interior to the SNR edges, the consistent appearance of the optical signatures of radiative shocks where indicators suggest that high preshock densities (and thus rapid cooling) are present, and the broad wings on H α in Balmer-dominated ("nonradiative") shocks, showing directly the transverse velocity dispersion in the postshock flows. *There is no question that the disturbance at remnant edges produces compressed high-temperature gas in an unresolved transition.*

Shock waves have also been studied for their acceleration of cosmic rays (CRs). It is found that acceleration by shocks associated with SNRs is a good candidate for the origin of the CRs with energies below 10^5 GeV (Blandford 1979; Drury 1983; Scholer 1985; Blandford and Eichler 1987). These theories predict that the CRs take most of the energy of a SN because of the high efficiency of CR production (Axford 1981; Heavens 1984). Much of the energy may be returned to gas flow via pV work following the epoch of acceleration.

Using the test particle approximation, it was found that shock waves are able to accelerate charged particles and generate power-law spectral distributions with an index depending only on the strength of the shock wave (Krysmky 1977; Axford, Leer, and Scadron 1977; Blandford and Ostriker 1978; Drury 1983; Blandford and Eichler 1987). The results were encouraging in that shock waves with gas compression factors slightly less than the maximum allowed (to adiabatic gas

shocks) seemed to be what were needed to reproduce the observed interstellar CR spectrum.

It was soon realized that this test particle approximation cannot be appropriate for strong shocks because the cosmic rays generated by the shock acquire most of the available pressure. Their dynamical effects on the shock cannot be neglected. Self-consistent models (Axford 1981; Drury and Völk 1981; Drury 1983) were then developed which added the CR pressure gradient to the driving terms for the gas. It was found that CRs should be present ahead of the gas subshock in a layer of characteristic thickness κ/U (diffusion coefficient/gas flow speed). In this layer the CR pressure gradient would gently preaccelerate and compress the (largely adiabatic) gas, softening the impulse received at the subsequent gas subshock. In some areas of parameter space the need for a gas subshock was removed altogether. The CRs dominated the pressure and in the limiting case approached an overall compression factor of $(\gamma_c + 1)/(\gamma_c - 1)$ or 7 for cosmic-ray adiabatic index $\gamma_c = 4/3$ in an entirely smooth transition. When the gas was treated adiabatically in the calculations, its pressure and temperature enhancements were then only $7^{5/3}$ and $7^{2/3}$, respectively, over the initial values. High temperatures found behind SNR shocks are not reproduced by such models.

In further study (McKenzie and Völk 1982; Völk, Drury, and McKenzie 1984), however, it became clear that there was an underlying inconsistency in the calculations. The CRs diffused in the gas but, more specifically, scattered off Alfvén waves which the CRs themselves generated in their rush to leave the acceleration region. The waves tend preferentially to be going opposite to the CR pressure gradient, and as a result there is net work done on them in their containment of that gradient. The net energy loss from the CRs by this wave generation tends to be small compared to the CR energy content. But it can be very large compared to magnetic and thermal energy densities, significantly altering the details of the structure. In particular, the assumption of the quasi-linear theory that the wave energy density is small compared to the ambient

magnetic pressure is invalidated. It is necessary to consider the possible damping of the generated waves under conditions of high amplitude (saturation).

Damping of the Alfvén waves is not well understood, although it has been suggested that nonlinear Landau damping (Völk 1986) and damping by phase mixing (Tataronis and Grossmann 1973) may be possible. In what follows, we assume that the waves dissipate very efficiently, somehow, when they are saturated (Völk, Drury, and McKenzie 1984) and that all this dissipated energy is released into the gas.¹ It is this model that offers some hope of generating gas of sufficient temperature to resemble the SNR observations and which we will explore for specific examples found in the Cygnus Loop.

Although time dependence of the acceleration remains an important and difficult issue (Dorfi 1985; Falle and Giddings 1987), it is likely that the dynamical effects of the cosmic-ray pressure can be important well before the acceleration of the highest energy particles. If dynamical effects have become important, then SNRs not only accelerate the cosmic rays, but should show signs of doing so. Hence our goal in this paper has been to see whether the observables of shock models, including cosmic-ray acceleration, might closely resemble those of pure gas shocks so that these signs of CR acceleration could have been overlooked. We chose the Cygnus Loop because of its different phases, its large apparent size, high brightness, low extinction in its direction, and extensive observations (Parker 1967; Cox 1972; Miller 1974; Hester, Parker, and Dufour 1983; Ku *et al.* 1984; Hester and Cox 1986; Raymond *et al.* 1988). We are aware of only one previous application of these theories to any SNR, Cas A where Morfill, Drury, and Aschenbach (1984) used the Völk, Drury, and McKenzie (1984) model to derive the bremsstrahlung emissivity and match it to the remnant's X-ray surface brightness.

In the following section we further discuss the models outlined above and derive the predicted downstream temperature for each. Section III presents the Cygnus Loop data and the application to it of the model, including wave dissipation. Heating rate and the ionization fraction structures are provided, along with an estimate of the cosmic-ray diffusion coefficient. Finally, the results are discussed in § IV.

II. SHOCK WAVE THEORIES

a) Downstream Temperatures

For a pure gas shock of speed U_1 in a medium of initial density $\rho_1 = mn_1$, with ionization fraction $f_1 = n_{e1}/n_1$, gas pressure P_{g1} , and sound speed $c_{s1} = [(5P_{g1})/(3\rho_1)]^{1/2}$, solution of the Rankine-Hugoniot relations (with Mach number $M_{s1} \equiv U_1/c_{s1}$) yields the inverse compression ratio

$$y_2 = \frac{n_1}{n_2} = \frac{U_2}{U_1} = \frac{M_{s1}^2 + 3}{4M_{s1}^2} \quad (1)$$

and the pressure enhancement factor

$$\bar{P}_{g2} \equiv \frac{P_{g2}}{P_{g1}} = \frac{5M_{s1}^2 - 1}{4}. \quad (2)$$

¹ An interesting alternative is that some of the energy is returned to the CRs, possibly to the electron component (Spangler 1985; Brooks and Pietrzyk 1987), which the theories tend otherwise to neglect.

The temperature enhancement factor follows from

$$\frac{T_2}{T_1} = \frac{n_1 + n_{e1}}{P_{g1}} \frac{P_{g2}}{n_2 + n_{e2}} = \frac{1 + f_1}{1 + f_2} y_2 \bar{P}_{g2}. \quad (3)$$

For strong shocks, appropriate to the Cygnus Loop, the simple limits are

$$y_2 \rightarrow \frac{1}{4}, \quad P_{g2} \rightarrow \frac{3}{4} \rho_1 U_1^2, \quad T_2 \rightarrow \frac{3mU_1^2}{16(1 + f_2)k}. \quad (4)$$

When cosmic-ray acceleration is efficient, and sufficient time has elapsed for it to become dynamically important, the Rankine-Hugoniot relations must be modified to take into account the CR pressure and energy flux. These relations yield new expressions for the gas pressure and inverse compression ratio (see Axford, Leer, and McKenzie 1982 for more details). Neglecting losses to wave generation, the relevant parameters, besides the sonic Mach number, are the ratio of upstream CR pressure to upstream gas pressure ($\delta \equiv P_{c1}/P_{g1}$) and the CR effective adiabatic index ($\gamma_c = 1 + E_c/P_c$, where E_c is the CR energy density). Defining a temperature ratio parameter independent of ionization changes,

$$T_0 \equiv \frac{(1 + f_2)T_2}{(1 + f_1)T_1} = \bar{P}_{g2} y_2, \quad (5)$$

we show the results for this parameter in Figure 1a ($\gamma_c = 4/3$) and Figure 1b ($\gamma_c = 1.5$) versus an effective Mach number $M_1(M_1^2 = M_{s1}^2/[1 + \gamma_c \delta/\gamma])$, where $\gamma = 5/3$ is the gas adiabatic index) for different values of δ . For $\gamma_c = 4/3$ the solution is triple valued at small δ and large Mach number. The upper solution pair is essentially the pure gas shock, which should always be a solution as $\delta \rightarrow 0$. Its presence or absence at finite δ depends on the detailed treatment of CRs and the degree of approach of the shock of interest to the absolute steady state. See Axford, Leer, and McKenzie (1982) and Drury (1983) for further discussion. Apart from the gas shock regime, the striking feature of this model is that the downstream temperature enhancement is small. For strong shocks dominated by cosmic rays, it is limited to the adiabatic compression factor

$$T_0 \rightarrow \left[\frac{\gamma_c + 1}{\gamma_c - 1} \right]^{2/3}. \quad (6)$$

The previous model assumes that CRs diffuse with respect to scatterers which are at rest relative to the gas. The scattering occurs through wave-particle interactions, and it has been shown (Völk and McKenzie 1981, 1982; Völk, Drury, and McKenzie 1984) that these waves play a major role in the shock dynamics. The pushing of the CR pressure gradient on the confining waves causes a preferential directionality of the latter, in effect giving the scatterers an upstream (or, in general, countergradient) motion at the Alfvén velocity ($V \equiv [B/(4\pi\rho)]^{1/2}$). The energy transfer rate per unit volume is then $V dP_c/dx$ from CRs to waves.

In the case at hand, the wave generation rate is huge and requires large damping if the diffusion approximation is to be valid. Waves must be present in order for the scattering to occur and acceleration to be efficient; therefore, we assume that saturation is reached when $\delta B/B \sim 1$ and that virtually all of the above power is available for dissipation. We consider only the case for which the wave power is rapidly (and locally) dissipated into the gas (Völk, Drury, and McKenzie 1984).

The Rankine-Hugoniot relations are unchanged from the

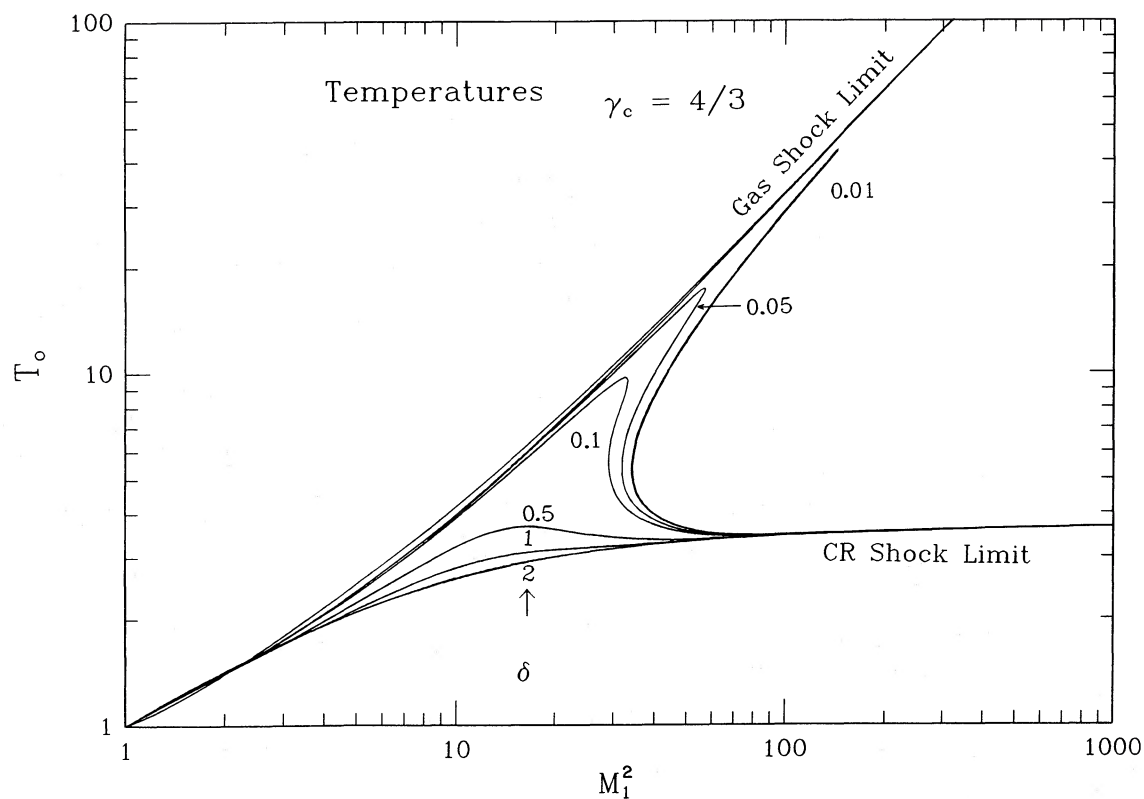


FIG. 1a

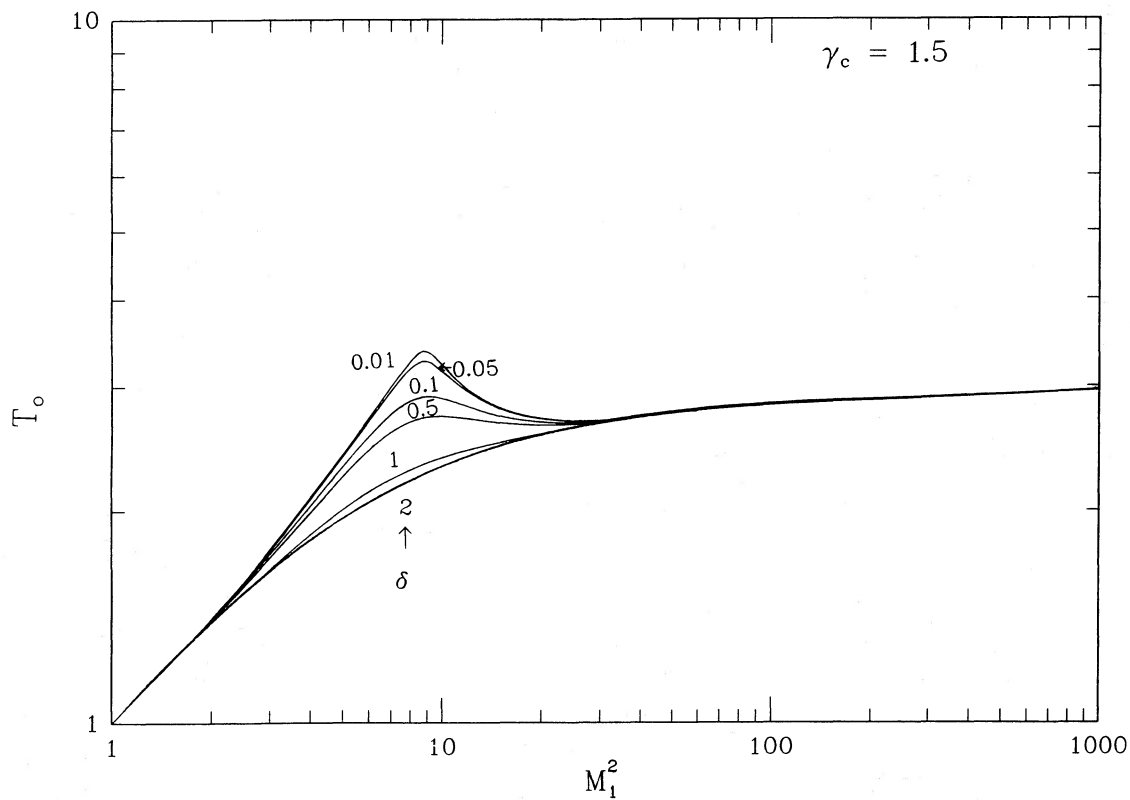


FIG. 1b

FIG. 1.—Temperature ratio with gas and cosmic rays only vs. an effective Mach number squared (see text for definition). The different curves correspond to different values of δ . (a) $\gamma_c = 4/3$: we note that there are two asymptotes, gas shock with a asymptotic behavior as M_1^2 and cosmic ray with a limit of $7^{2/3}$. In this case the temperature is triple valued for $\delta \leq 0.1$ and $M_1 \geq 5.5$. (b) $\gamma_c = 1.5$: notice the drastic change in the triple valuedness of the temperature; reduced gas shock effects and smaller downstream temperatures.

previous model; the only changes being in the cosmic-ray flux equation in which the bulk velocity is $(U - V)^2$ and in the energy equation for the gas. The CR flux is

$$F_c = \frac{\gamma_c}{\gamma_c - 1} (U - V) P_c - \frac{\bar{\kappa}}{\gamma_c - 1} \frac{dP_c}{dx}, \quad (7)$$

where $\bar{\kappa}$ is the effective diffusion coefficient, while the gas equation including the possibility of radiation is

$$\frac{U\rho^\gamma}{\gamma - 1} \frac{d}{dx} \left(\frac{P_g}{\rho^\gamma} \right) = V \frac{dP_c}{dx} - L(T)m_e. \quad (8)$$

The radiative cooling coefficient, $L(T)$, is a function of at least the temperature (Cox 1972; Raymond 1976). The high value of $L(T)$ around 10^5 K (e.g., Raymond, Cox, and Smith 1976) establishes a minimum required heating rate for promotion of the gas to higher temperatures. In our initial investigations below, we neglect cooling in the calculation, checking its post facto magnitude for consistency.

For a strong shock dominated by cosmic rays, we expect the CR pressure to evolve as $P_c \approx (1 - y)\rho_1 U_1^2$, where y is the inverse compression anywhere in the structure. The ultimate compression should approach $1/y_f = (\gamma_c + 1)/(\gamma_c - 1)$. Within the structure $U = U_1 y$, $V = V_1 y^{1/2}$ (parallel B), $\rho = \rho_1 y^{-1}$. In this limit the integral of the gas energy equation (8) yields

$$(1 + f_2)T_2 = \left\{ \frac{4}{13} y_f [y_f^{-5/3} - y_f^{1/2}] \right\} \frac{mU_1 V_1}{k}. \quad (9)$$

The expression within the curly bracket equals 1.11, 0.87, 0.74 for $\gamma_c = 4/3, 1.5, 5/3$, respectively. Comparing this result with equation (4) for a pure gas shock, the strong CR-dominated shocks are seen to be less efficient for heating gas by a factor of order $5V_1/U_1$. In principle, any postshock temperature can be reached in this model, although higher shock velocities are required than for the gas shock.

The Alfvén velocity introduces a new parameter into this model, generally taken as $\beta = 8\pi P_{g1}/B_1^2$. With this, the above approximation to the downstream temperature can be expressed in terms of the corresponding temperature enhancement factor

$$T_0 = \frac{(1 + f_2)T_2}{(1 + f_1)T_1} \approx \frac{A M_{s1}}{(\beta)^{1/2}}, \quad (10)$$

where $A = 2.03, 1.59, 1.35$ for $\gamma_c = 4/3, 1.5, 5/3$, respectively. This can be compared with the results of complete model calculations shown in Figures 2a-2c for $\gamma_c = 4/3$ and Figure 3a for $\gamma_c = 1.5$. The agreement is excellent at large M_{s1} . In addition, the pure gas shock result, $T_0 \approx 5M_{s1}^2/16$ for strong shocks, provides an upper approximate envelope to the family of curves.

At low Mach numbers the T_0 results show a wealth of complexity that depends sensitively on δ, β , and γ_c . For the most part, study of this detail is outside the scope of this paper. We have, however, included dotted lines indicating the parameter range within which the overall shock structure includes a gas

² In a true steady flow, the CR pressure gradient downstream of the shock is zero. The vanishing of the diffusion flux leads to vanishing of the slip velocity between gas and waves so that, in principle, one should set $V = 0$ in equation (7) in this regime. Under less steady conditions, when there is a net downstream diffusion away from the shock, one might expect to replace $-V$ by $+V$ in this regime. Neglect of this effect damages the simple (Völk, Drury, and McKenzie 1984) model at low Mach numbers.

subshock. Outside this range, the transitions are completely smooth.

b) Caveats

The steady state can be a reasonable description only if the age of the SNR greatly exceeds the acceleration time scale of the bulk of the cosmic rays. The characteristic time scale for the acceleration process is

$$t_c = \frac{\bar{\kappa}}{4U^2}. \quad (11)$$

From simple kinetic theory, $\bar{\kappa} \sim \lambda c/3$, where λ is the mean free path and c is the CR speed. From SNR evolution in the adiabatic phase (in a homogeneous medium) we have $t = 2R/(5U)$, where R is the SNR radius; hence $t_c/t \approx (5\lambda c)/(24RU)$. Thus $t \gg t_c$ requires $\lambda \ll 5RU/c$. Since $U \ll c$, the CR mean free paths must be extraordinarily small. Similarly, the characteristic diffusion length $x_c = \bar{\kappa}/(2U) = 2Ut_c$ has a ratio $x_c/R = 2Ut_c/R \sim t_c/t$. Hence, the use of plane-parallel geometry is automatically satisfied whenever the steady state description is valid.

A rough estimate of t_c is obtained by noting that the gyroradius r_g provides a lower limit to the particle mean free path for particle-wave interaction. For an ambient magnetic field of $5 \mu\text{G}$, and for the moment using γ and β in their relativistic contexts, we have

$$t_c \sim 0.5\gamma\beta \left(\frac{\lambda}{r_g} \right) \left(\frac{100 \text{ km s}^{-1}}{U} \right)^2 \text{ yr}. \quad (12)$$

One is encouraged to suppose t_c/t could be sufficiently small, but caution is in order.

There is some evidence that in the general interstellar medium the diffusion coefficient must be about 10^{28} – $10^{29} \text{ cm}^2 \text{ s}^{-1}$ in order to provide particle escape after diffusion of 1 kpc in 10^7 yr (Ginzburg and Syrovatskii 1964; Ginzburg and Ptuskin 1976). This corresponds to $(\lambda/r_g) \sim 10^6$ – 10^7 . In the general interplanetary medium $\bar{\kappa}$ is about 10^{20} – $10^{21} \text{ cm}^2 \text{ s}^{-1}$ for 1 MeV particles in a magnetic field of $50 \mu\text{G}$. (Toptygin 1985), making $(\lambda/r_g) \sim 10$ – 100 .

In addition, we must suppose that the initial buildup of the cosmic rays takes place in a strong, gas-dominated shock with compression factor 4. It is straightforward in that case to demonstrate that for $\bar{\kappa}$ independent of energy the CR pressure accumulates *linearly* in time. The process pushes toward a power-law spectrum downstream

$$\frac{dn}{dE} = \frac{4E_0 S}{U_1} E^{-2}, \quad (13)$$

where E_0 is the particle injection energy and S is the source rate of fresh particles. The power law is constructed in time, from low energy up to a maximum which behaves as $E_{\text{max}} \sim E_0 \exp(\alpha t/t_c)$. The downstream CR pressure is then

$$P_{c2} \sim \frac{1}{3} \int_{E_0}^{E_{\text{max}}} E \frac{dn}{dE} dE = \frac{4E_0 S}{3U_1} \ln \left(\frac{E_{\text{max}}}{E_0} \right) \sim \left(\frac{4\alpha E_0 S}{3U_1} \right) \frac{t}{t_c}. \quad (14)$$

The parameter α is approximately $\frac{1}{3}$ (Cox and Boulares 1988); the time t is the effective age of the shock wave system.

If the injection source were merely swept-up cosmic rays, then $P_{c1} \sim E_0 S/(3U_1)$ and $P_{c2}/P_{c1} \sim 4\alpha t/t_c$. Roughly speak-

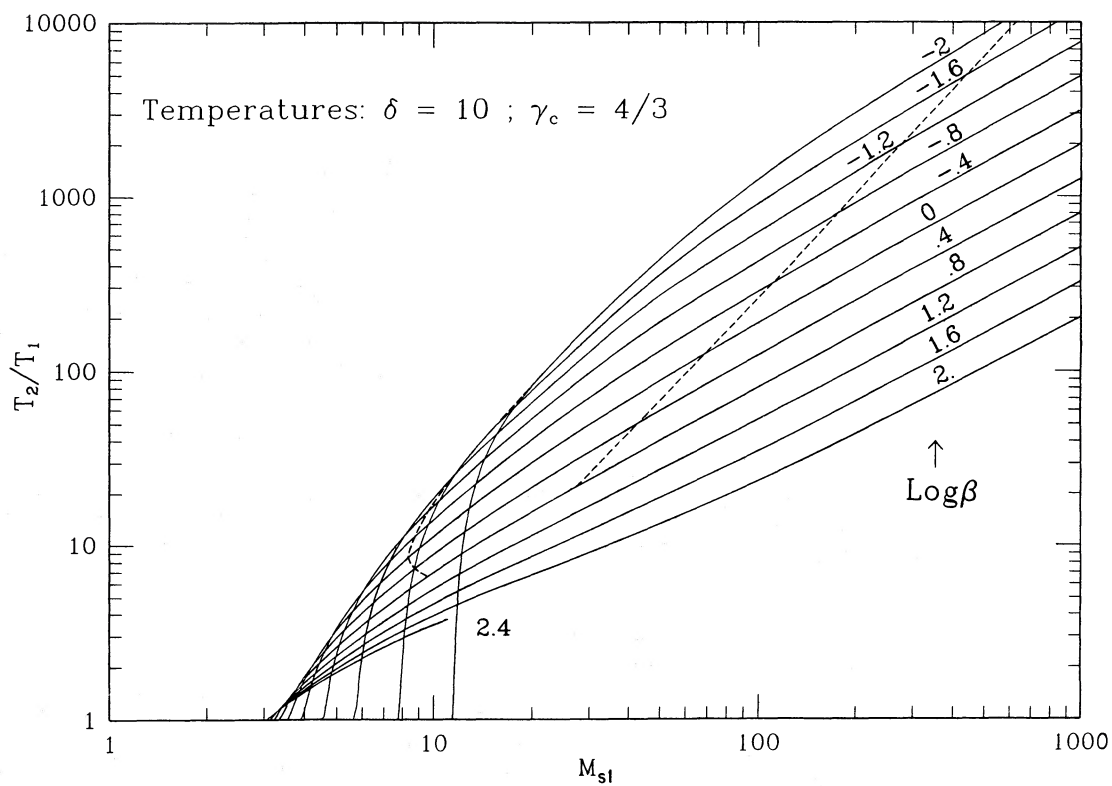


FIG. 2a

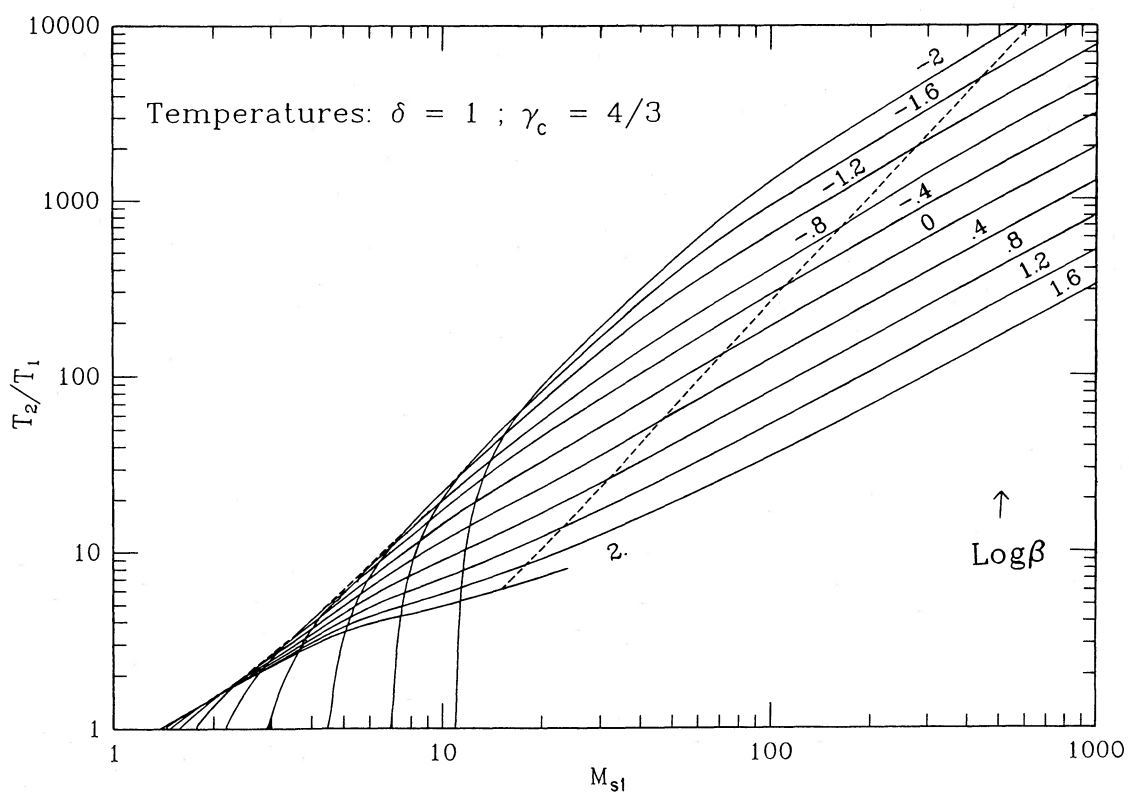


FIG. 2b

FIGS. 2a-2c.—Temperature ratio T_2/T_1 vs. the sonic Mach number for (a) $\gamma_c = 4/3$ and $\delta = 10$, (b) $\delta = 1$, and (c) $\delta = 0.01$, for different values of $\log(\beta)$. The dashed lines correspond to the lower and upper limits within which the solutions admit a subshock. Note the structure variation for the low values of both the temperature ratios and the Mach number. For $\delta = 0.01$, the gas shock asymptote (the upper curve at low Mach number) corresponds to high values of β .

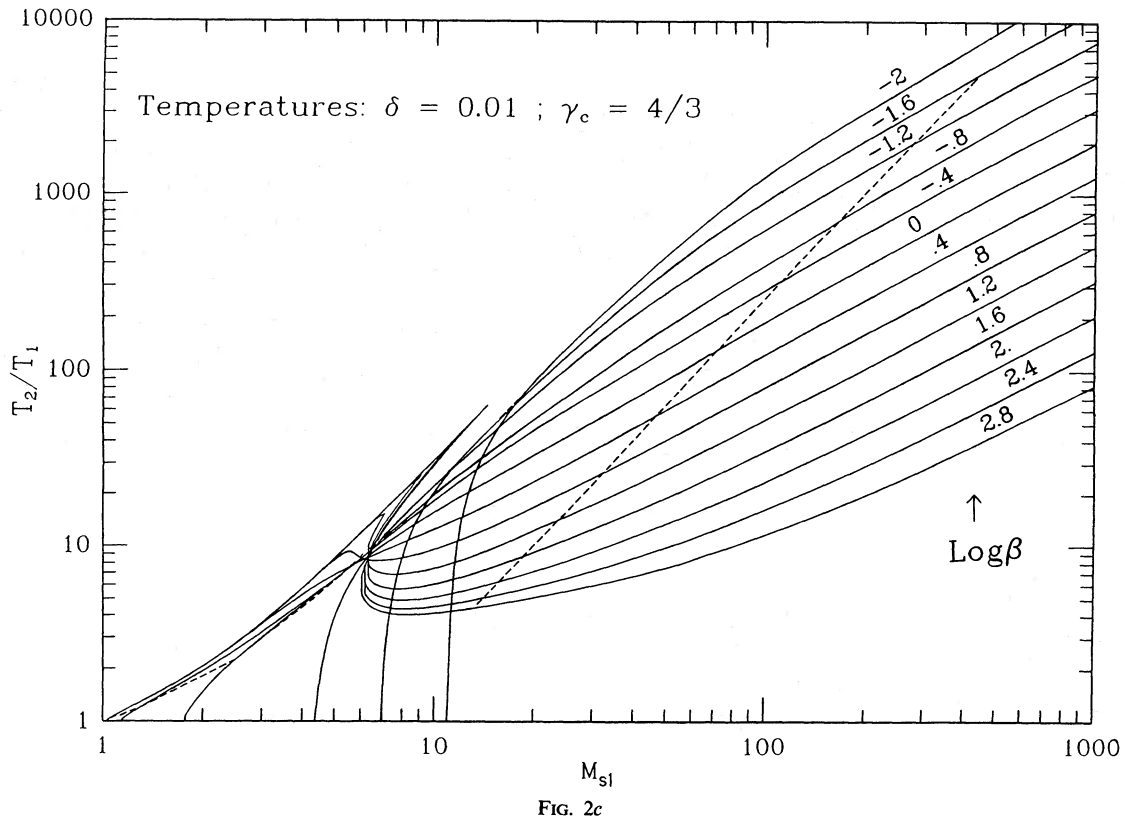


FIG. 2c

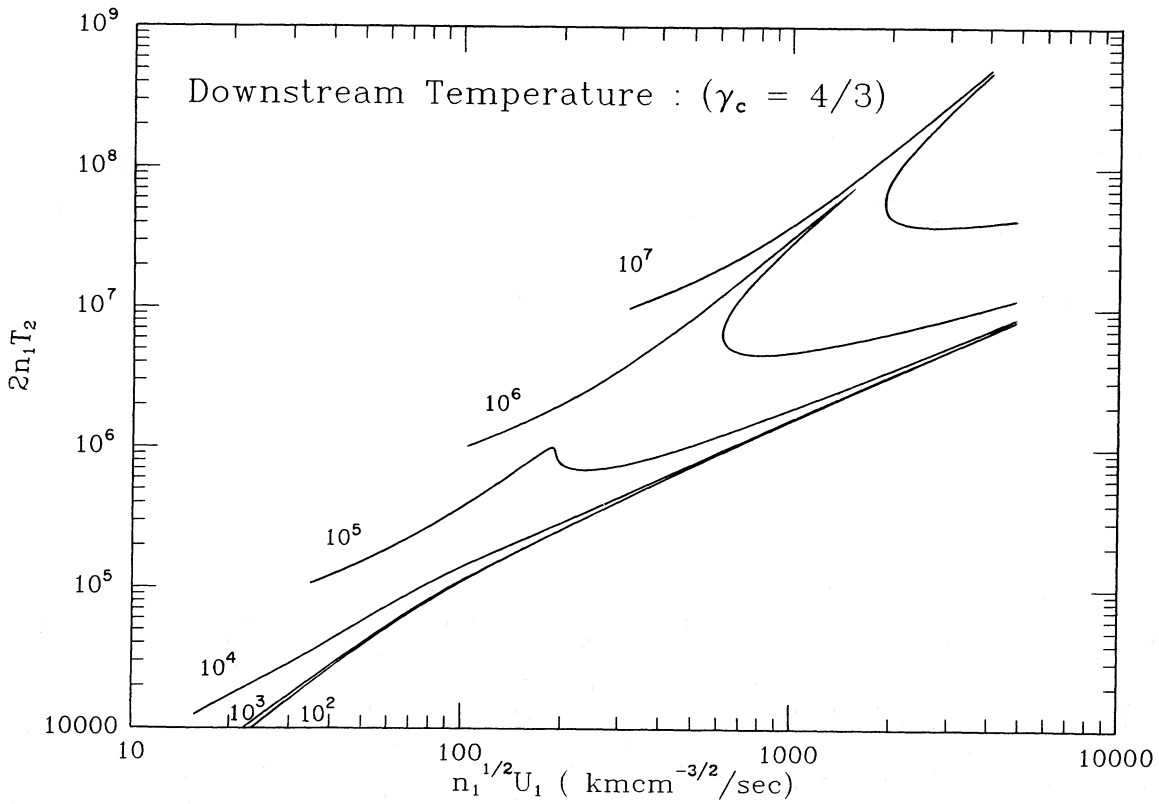


FIG. 2d

FIG. 2d.— $2n_1T_2$ ($\text{cm}^{-3} \text{K}$) vs. $n_1^{1/2}U_1$ for different values of P_{01} ($\text{cm}^{-3} \text{K}$). The upstream gas pressure becomes important only for values larger than $\sim 10^4 \text{ cm}^{-3} \text{K}$, and its actual value in the general ISM does not exceed $10^5 \text{ cm}^{-3} \text{K}$ for which the downstream temperature is single valued. Note also that the curves are independent of the upstream density. Calculation assumes $B_1 = 5 \mu\text{G}$, $P_{c1} = 4.3 \times 10^{-13} \text{ dyn cm}^{-2}$.

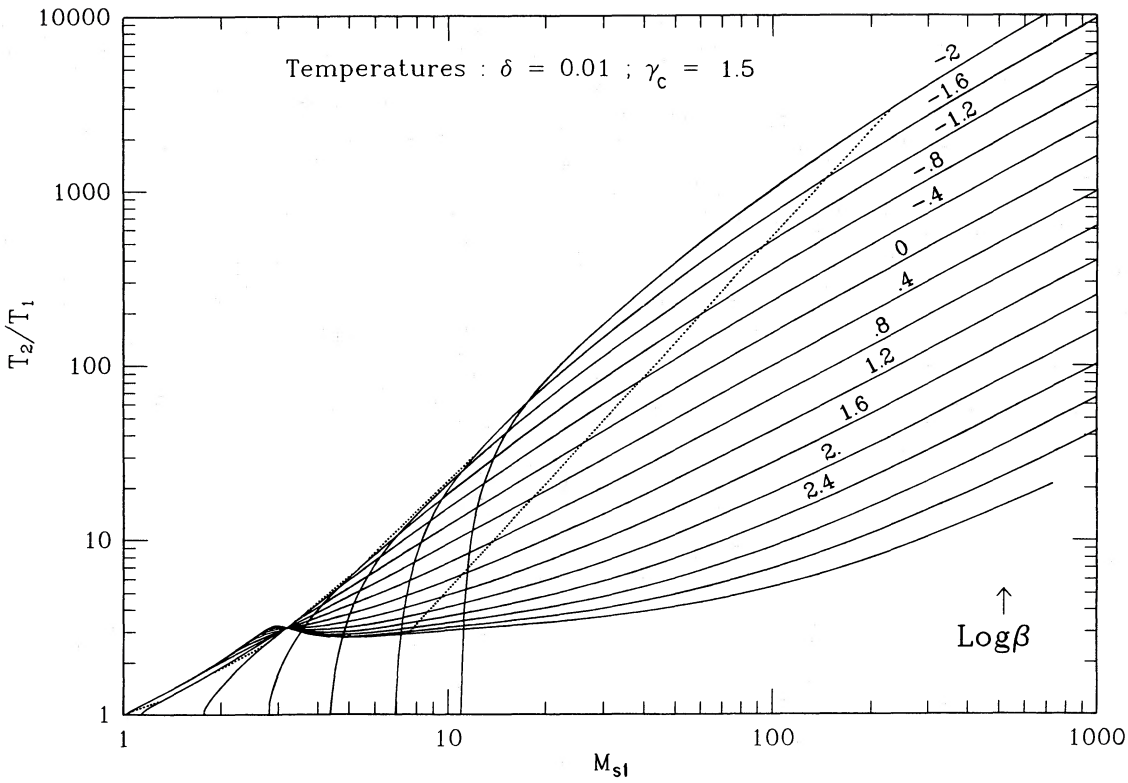


FIG. 3a

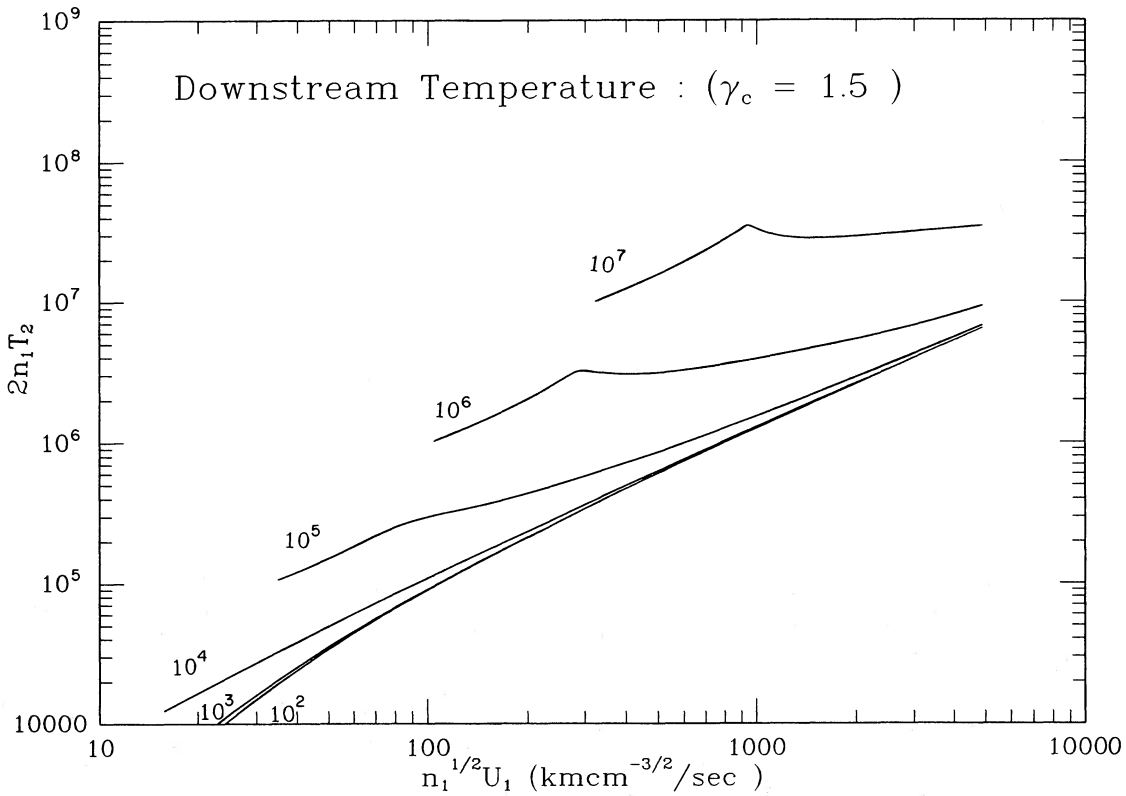


FIG. 3b

FIG. 3.—(a) Same as in Fig. 2c for $\gamma_c = 1.5$ with $\delta = 0.01$. (b) Same as in Fig. 2d for $\gamma_c = 1.5$.

ing, the diffusion of cosmic rays in the neighborhood of the shock constructs the power law from an arbitrary injection spectrum, but $t \gg t_c$ is required to extend the spectrum to high energy and dynamical significance. In addition, t/t_c is approximately the pressure enhancement factor over what would have been present from the injection process alone.

For CR to be dynamically important in the Cygnus Loop, $P_{c2} \sim 10^{-9}$ dyn cm $^{-2}$ (Raymond *et al.* 1988), whereas $P_{c1} \leq 10^{-12}$ dyn cm $^{-2}$, requiring an overall enhancement factor of over 10^3 . Either $t/t_c \geq 10^3$ is needed or there is a copious injection process within the shock. Possible forms of the latter have been studied by Eichler (1979) and others, but the anticipated rate is unknown. What is known independently, however, is that fresh injection must dominate reacceleration by a large factor in order for the observed higher energy CR to be, on average, younger than the lower energy ones (e.g., Wandel *et al.* 1987).

In summary, it is possible that the Cygnus Loop shocks (effective age $t \sim 10^4$ yr, $U \sim 10^2$ – 10^3 km s $^{-1}$) can have had time to approach CR domination. For example, $\lambda/r_G \sim 10^2$, $U \sim 300$ km s $^{-1}$, and $\gamma\beta \sim 2$ yield $t_c \sim 10$ yr. If the injection mechanism channels 1% of the total shock energy into cosmic rays, diffusive enhancement will bring domination in 10^3 yr. Even with no injection other than the inflowing CR, it is possible that the CR pressure has become important, but it is less likely that the steady state has been reached. An understanding of the CR injection mechanism in gas-dominated shocks is of critical importance.

In addition to the time scale problems above, we are not convinced that either the quasi-linear diffusion approximation or the assumption of quasi-parallel geometry are entirely appropriate in this context. They are, however, the models available.

III. APPLICATION TO THE CYGNUS LOOP

a) *Cygnus Loop Data*

The Cygnus Loop is a filamentary supernova remnant $\sim 3^\circ$ in diameter and thought to be about 770 pc away. The optical filaments are wavy sheets of recently shocked gas seen edge-on (e.g., Poveda and Woltjet 1968; Hester 1987). The loop has been studied in many radiation bands: in radio continuum (Dickel and Willis 1980), 21 cm (DeNoyer 1974), optical (Miller 1974; Hester, Parker, and Dufour 1983), UV (Benvenuti, Dopita, and D'Odorico 1980; Raymond *et al.* 1988), and X-ray (Gronenschild 1980; Ku *et al.* 1984; Charles, Kahn, and McKee 1985; Hester and Cox 1986). The observations in the optical seem to indicate that some regimes of the loop are in the late radiative stages (Cox 1972). The depth of the radiating material is several times its width, perhaps as much as a factor 10 or more (Parker 1964; Raymond *et al.* 1988). The very high [O III] temperature and the much lower [O II], [N II], and [S II] temperatures are unique to the Cygnus Loop and similar remnants (Osterbrock and Dufour 1973), and are, along with the UV observations (Benvenuti, Dopita, and D'Odorico 1980), the most convincing evidence that shock ionization is taking place. However, the X-ray observations indicate a more symmetrical remnant, with a hotter interior ($T \sim 2.4 \times 10^6$ K), in a rather adiabatic behavior. The X-ray remnant is composed of a hot interior, a bright limb, and indications of an extended emitting region of low surface brightness beyond the shell (Ku *et al.* 1984; Charles, Kahn, McKee 1985). This could be interpreted as a shock wave

with a smooth CR-driven precursor, a gas subshock, and a hot postshock region. This is the normal structure of the CR shock models. According to Woltjer (1972), the early measurements of X-ray intensity could be fitted by a power law with an exponent of 2.2 ± 0.3 or by an exponential ($kT = 0.4$ keV). Recently, Ku *et al.* (1984) and Charles, Kahn, and McKee (1985) found the spectrum to be dominated by thermal emissions from line-emitting atoms: O VIII, O VII, N VI, N VII, C VI, and Fe XVII. It is still possible that there is a weaker non-thermal component from particles accelerated in the neighborhood of the shock.

The observations in the optical have been compared to the X-ray data (Ku *et al.* 1984; Hester and Cox 1986) and to the radio data (Ku *et al.* 1984; Straka *et al.* 1986). Both comparisons yield a correlation on large scales, but not always on small scales. There are, however, two extended bright X-ray regions (east and west limbs), which are associated with optical emission, with the X-ray emission coming from a thin zone located immediately behind the much thinner sheetlike locus of optical emission. Ku *et al.* (1984) concluded that according to the X-ray data the Cygnus Loop sits in a low-density (≤ 0.1 cm $^{-3}$), warm (10^4 K) interstellar medium (ISM) which contains many clouds ($\leq 10^3$ K) that when shocked radiate in the optical. Hester and Cox have shown that this point of view is unrealistic. They suggested instead that in these zones of high correlation (optical and X-ray) and great X-ray brightness, the latter derives from doubly shocked gas. The reflection of the shock wave off large dense clouds needed for the optical emission provides an intensely heated very high pressure zone, exactly as required. In what follows, we shall be ignoring these bright regions, concentrating on the diffuse X-ray shell away from bright optical emission. The radio data indicate a better, although not complete, correlation with the optical observations, particularly the filaments which are bright in H α . The radio emission is generally associated with synchrotron radiation where the enhancement may be due partly to the compression of the frozen magnetic field lines and also to the shock acceleration of relativistic particles (Straka *et al.* 1986). Recently, Raymond *et al.* (1988) have been able to measure the ram pressure ($\sim 1.9 \times 10^{-9}$ dyn cm $^{-3}$) behind the shock of the Spur (a bright feature located at the southeast of the Loop, and so named by Hester, Parker, and Dufour [1983]). They found that the ram pressure is an order of magnitude larger than the thermal pressure in the recombination zone. This suggests the possibility of a large nonthermal pressure which may be associated either with a large magnetic field or a dominant cosmic-ray pressure due to the shock acceleration process. Much of the effect could derive from the transient drop in thermal pressure in rapidly cooling gas during shell formation (Straka 1974).

Most of the models of the Cygnus Loop have been confined to purely gas shocks (Cox 1972; Raymond 1979; Shull and McKee 1979; Cox and Raymond 1985) for radiative or non-radiative conditions. The importance of the nonthermal pressures in the evolution of the supernovae remnants, like the Cygnus Loop, was not taken seriously until the latest results of Raymond *et al.* (1988), although the cosmic-ray literature has been emphasizing it for more than a decade (Parker 1966; Axford, Leer, and Scadron 1977; Axford 1981; Völk 1984). We consider three sets of parameters, the gas shock interpretations of which are given in Table 1. They correspond to three states in the Cygnus Loop, which are, respectively, the cloudless X-ray bright regions (north and south), the intermediate

TABLE 1
STANDARD PARAMETERS OF THE CYGNUS LOOP

Parameter	Set Number 1 (X-Ray)	Set Number 2 (H α)	Set Number 3 (Radiative)
Density (cm $^{-3}$), n_H	0.16	1	8
Ionization factor, f_1	0.5	0.5	1
Temperature, T_1 (K)	8000	8000	8000
Magnetic field, B_1 (μ G)	5	5	5
Temperature, T_2 (K)	2.4×10^6	3.5×10^5	1.5×10^5
CR pressure, P_{c1} (CGS)	4.3×10^{-13}	4.3×10^{-13}	4.3×10^{-13}
Temperature ratio, T_0	400	60	20
Gas pressure, P_{g1} (cgs)	2.65×10^{-13}	1.6×10^{-12}	1.8×10^{-11}
Shock velocity, U_1 (km s $^{-1}$)	400	150	100
Sonic Mach number, M_{s1}	30	10	6

regions (nonradiative or “Balmer-dominated” shocks), and the optically bright regions (southwest and northeast) which are mostly radiative.

The properties of ambient gas, cosmic rays (δ , γ_c), and magnetic field (β) far upstream are uncertain. However, the apparent presence of gas shocks (or subshocks) in the Cygnus Loop and the approximate equality between the energy densities of cosmic rays, magnetic field, and thermal gas in the general ISM restricts the choice of the values of δ and β . We will assume that the CR pressure far upstream corresponds to the known CR energy density in the general ISM (i.e., $P_{c1} = \epsilon_c/3 = 4.3 \times 10^{-13}$ dyn cm $^{-2}$) (Spitzer 1978; Ginzburg and Ptuskin 1985; Webber 1987), and the magnetic field is about 5 μ G (Sofue, Fujimoto, and Wielebinski 1986; Troland and Heiles 1986).

b) Applications

The cases considered have temperature ratios between 20 and 400; the Axford, Leer, and McKenzie (1982) model is unable to provide those ranges because of the inefficiency in the heating of the gas. This is, as we saw earlier, due to neglect of wave slip. However, the Völk, Drury, and McKenzie (1984) model is able to produce high temperatures both in the precursor of the shock wave and downstream.

In going to a drastic new model for the three types of shock regions, one must take care about the parameters actually constrained by observations, independent of the gas shock interpretations. In the radiative part of the Cygnus Loop, the ram pressure is known (Raymond *et al.* 1988) providing $n_0 v_0^2$; in the nonradiative shocks (H α emission) the number flux $n_0 v_0$ has been estimated (Raymond *et al.* 1983); and finally, in the X-ray emitting region, the downstream density is derived from the X-ray brightness (Ku *et al.* 1984). The downstream temperatures are known for all shocks, from UV spectra for the radiative shocks, line width for Balmer emission shocks, and X-ray spectra for X-ray shocks.

We explored the downstream gas pressures by varying the upstream density, gas pressure, and shock velocity. We found the quantity $n_1(1 + f_2)T_2$ to be independent of the density if it is plotted against $n_1^{1/2}U_1$ with the upstream gas pressure as a parameter. Figures 2*d* and 3*b* show the results for two cases of γ_c . For γ_c of 4/3 there are triple-valued solutions at high upstream pressures and high Mach numbers; although, for the most likely upstream pressures ($\leq 10^5$ cm $^{-3}$ K), the results are single valued. For $\gamma_c = 1.5$ there are no multiple solutions for $P_{g1} < 10^7$ cm $^{-3}$ K (Fig. 5*b*, below). These two figures, along with corresponding density information, form the basis for our interpretations below.

i) X-Ray-Emitting Shock

Representative values of the downstream density and temperature are 0.64 cm $^{-3}$ and 2.4×10^6 K, respectively (Ku *et al.* 1984), while the upstream temperature is assumed to be 10^2 – 10^4 K. Here, we needed to solve iteratively for the appropriate shock velocity and upstream density which give the correct observed quantities. We found that an upstream density of 0.106 cm $^{-3}$ and a shock velocity of 1110 km s $^{-1}$ are required for $\gamma_c = 4/3$, and 0.136 cm $^{-3}$ and 1455 km s $^{-1}$, respectively for $\gamma_c = 1.5$. The uncertainty in preshock temperature was of no consequence as can be seen by comparing the $P_{g1} = 10^2$ – 10^4 cm $^{-3}$ K curves in Figures 2*d* and 3*b*. We assumed that the upstream and downstream ionization fractions are 0.5 and 1, respectively. As anticipated from the approximate postshock temperature calculations of equation (9), the velocities above are about 3 times larger than those of the conventional gas shock interpretation (~ 300 – 400 km s $^{-1}$) (see Tuohy, Nousek, and Garmire 1979).

The spatial structure of the velocity, gas pressure, and CR pressure are shown in Figures 4*a* and 4*b* in which ξ is a dimensionless spatial variable ($d\xi \equiv [U_1 dx]/[\bar{\kappa}]$). We see that although the structures are mostly smooth, they are also very steep; all the change occurs within $\Delta\xi = 3$ – 4 . \bar{P}_c and \bar{P}_g are normalized to the total momentum flux. The downstream ratio of CR to gas pressure is ~ 3.5 , and the jump compression ratio is only ~ 1.35 , while the total compression ratio is about 6.05 for $\gamma_c = 4/3$. For $\gamma_c = 1.5$, the whole structure is smooth (Fig. 4*b*), lying just outside the jump domain.

ii) The Nonradiative Balmer-Dominated Shocks

In this case our representative constraints are a downstream temperature of 3.5×10^5 K from the H α line width and particle flow of 170×10^5 cm $^{-2}$ s $^{-1}$ (Raymond *et al.* 1983). An iterative method using Figures 2*d* and 3*b* yields an upstream density of 0.47 cm $^{-3}$ and a shock velocity of 365 km s $^{-1}$ for $\gamma_c = 4/3$; for $\gamma_c = 1.5$ the values are 0.42 cm $^{-3}$ and 400 km s $^{-1}$, respectively. These densities are about half the gas shock ones (~ 1 cm $^{-3}$), while the velocities are about double (~ 170 – 210 km s $^{-1}$) (e.g., Raymond *et al.* 1983). The spatial structure of the velocity, gas pressure, and CR pressure are shown in Figures 5*a* and 5*b*. Similar to the previous case, the structure admits a weak jump for $\gamma_c = 4/3$, and is smooth for $\gamma_c = 1.5$.

iii) Radiative Shocks

The radiative shock may not be well modeled by the present theory because the cosmic-ray diffusion should interact with the postshock cooling and recombination regions as well as with the initial shock. We can proceed, however, in the limit of

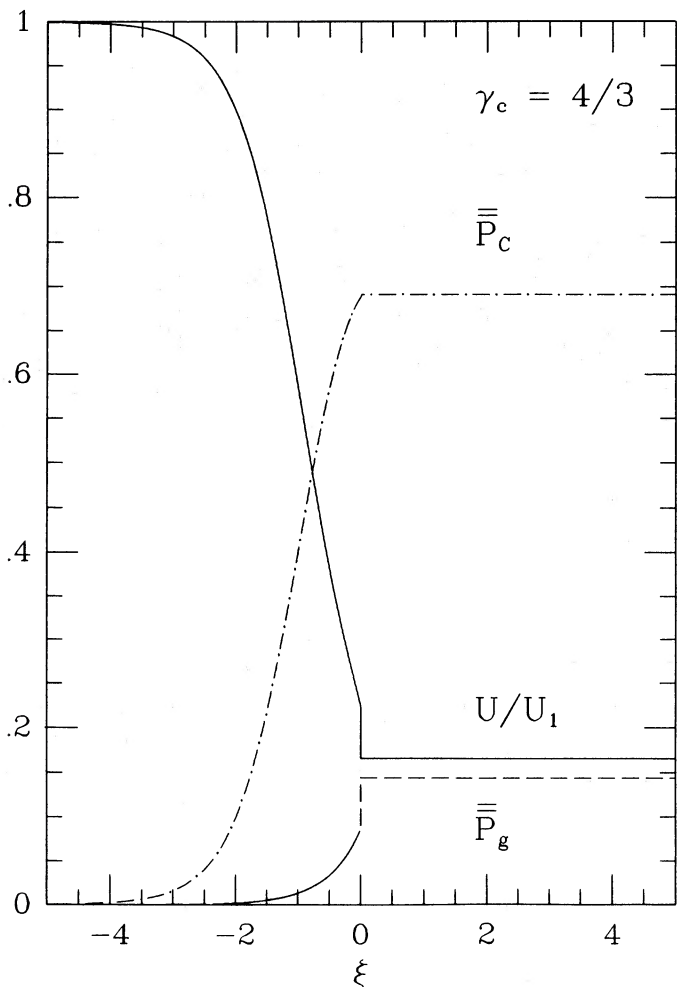


FIG. 4a

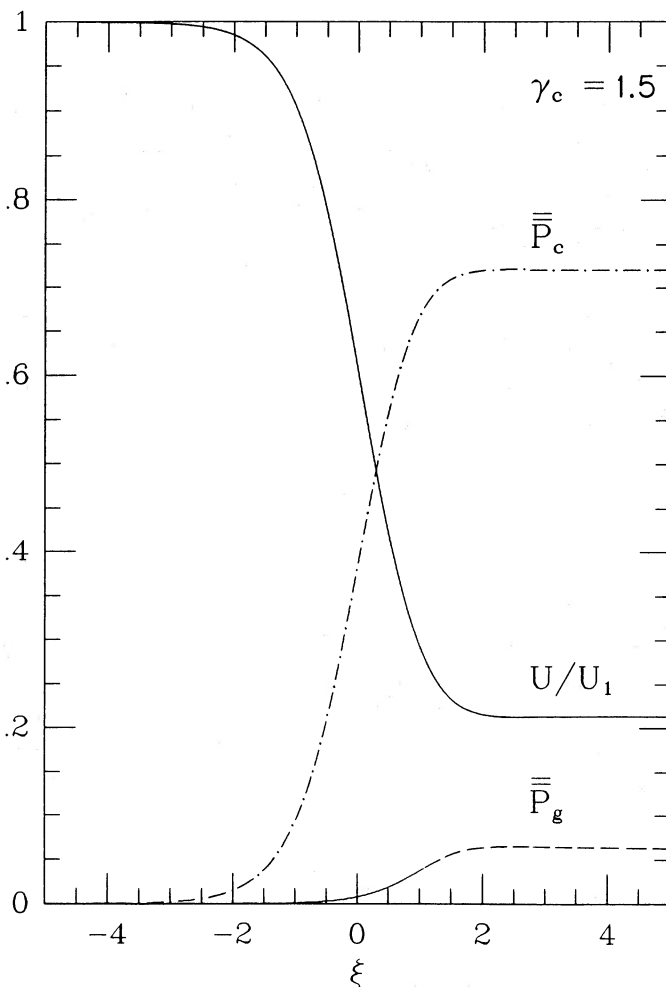


FIG. 4b

FIG. 4.—Spatial structure (ξ) of the velocity U/U_1 , gas pressure \bar{P}_g , and the cosmic-ray pressure \bar{P}_c (see text) of the X-ray shock. (a) The case of $\gamma_c = 4/3$. (b) The case of $\gamma_c = 1.5$. The former case exhibits a jump whereas the latter does not.

small CR mean free path, to explore just the initial shock. We are particularly interested to see whether the ratio of ram pressure to thermal pressure can be around 7 as observed by Raymond *et al.* (1988). The ram pressure was measured by a new technique and was found to be around 1.9×10^{-9} dyn cm^{-2} . Therefore, we will use this ram pressure and the post-shock temperature 1.5×10^5 K to derive the upstream density and the shock velocity. The upstream ionization fraction is measured to be 1 and is due to photoionization from UV produced on the downstream side of the shock. From Figure 2d we find a density of 1.5 cm^{-3} , a shock velocity of 230 km s^{-1} , and a total compression ratio of 5.75 for $\gamma_c = 4/3$. Similarly, for $\gamma_c = 1.5$ (Fig. 3b) we find 1.25 cm^{-3} , 260 km s^{-1} , and 4.45, respectively. The densities are much lower than the previously inferred ones ($\sim 8 \text{ cm}^{-3}$), while the velocities are about a factor 2.4 greater than the pure shock values ($70\text{--}130 \text{ km s}^{-1}$) (e.g., Raymond *et al.* 1983). The spatial structures are shown in Figures 6a and 6b. Some results on the three cases are summarized in Table 2.

iv) Heating Rates, Ionization Fraction, and Temperature Structures

We now must investigate the heating rate to see whether it is indeed sufficient to overwhelm radiative cooling so that high

temperatures can be reached. The dissipative heating rate (in $\text{ergs cm}^{-3} \text{ s}^{-1}$) is given by

$$h = V \frac{dP_c}{dx} = \left(\frac{P_{g1} U_1^2}{M_{A1} \bar{\kappa}} \right) y^{1/2} \frac{d\bar{P}_c}{d\xi}; \quad (15)$$

the rate per atom is then

$$\frac{h}{n} = \left(\frac{P_{g1} U_1^2}{n_1 \kappa_0 M_{A1}} \right) \frac{y^{3/2}}{F} \frac{d\bar{P}_c}{d\xi} = \left(\frac{h}{n_0} \right) \frac{1}{F}, \quad (16)$$

with $\bar{\kappa} = \kappa_0 F$, where $\kappa_0 = cr_G/3$ and is about $10^{22} \text{ cm}^2 \text{ s}^{-1}$ for a mean free path λ equal to the gyroradius r_L of a 1 GeV particle in a $5 \mu\text{G}$ magnetic field; and F is the factor (λ/r_G) which may be between 1 and 10^6 . The quantity $(h/n)_0$ is shown in Figures 7a–7c as a function of ξ for the X-ray, nonradiative, and radiative shocks, respectively. This heating rate is the largest for the X-ray shock in which it can attain $10^{-16} \text{ ergs s}^{-1} \text{ atom}^{-1}$ if F is equal to 1. This is very large compared to the required heating of the interstellar medium which is about $10^{-25} \text{ ergs s}^{-1} \text{ atom}^{-1}$. The maximum cooling rate which must be overwhelmed is of order $10^{-21} n_e \text{ ergs s}^{-1} \text{ atom}^{-1}$ (Raymond, Cox, and Smith 1976), which should be easy for the X-ray shock given $F \leq 10^5$, and for the others as well if

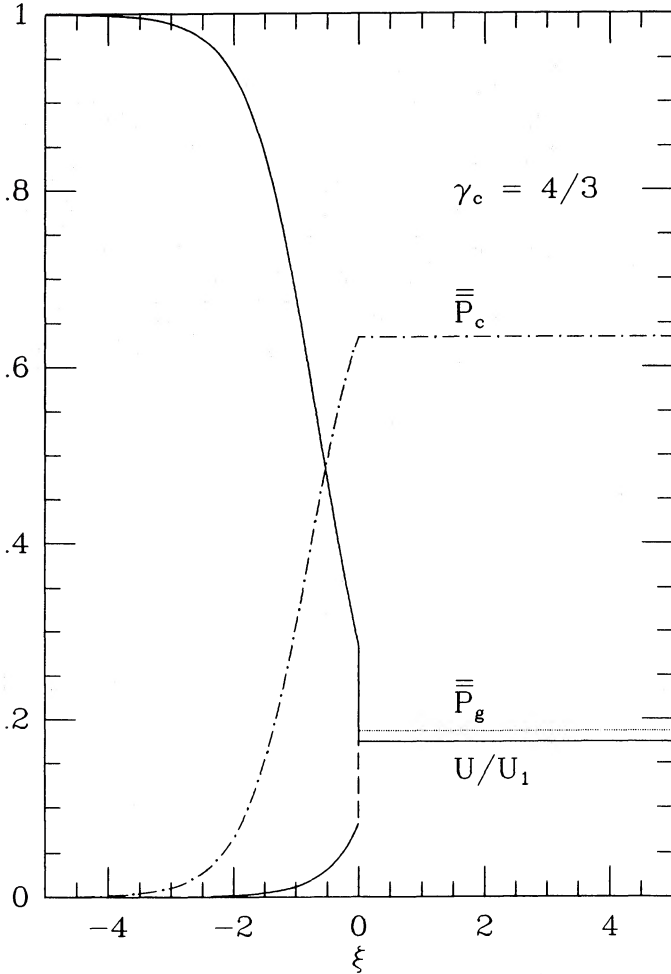


FIG. 5a

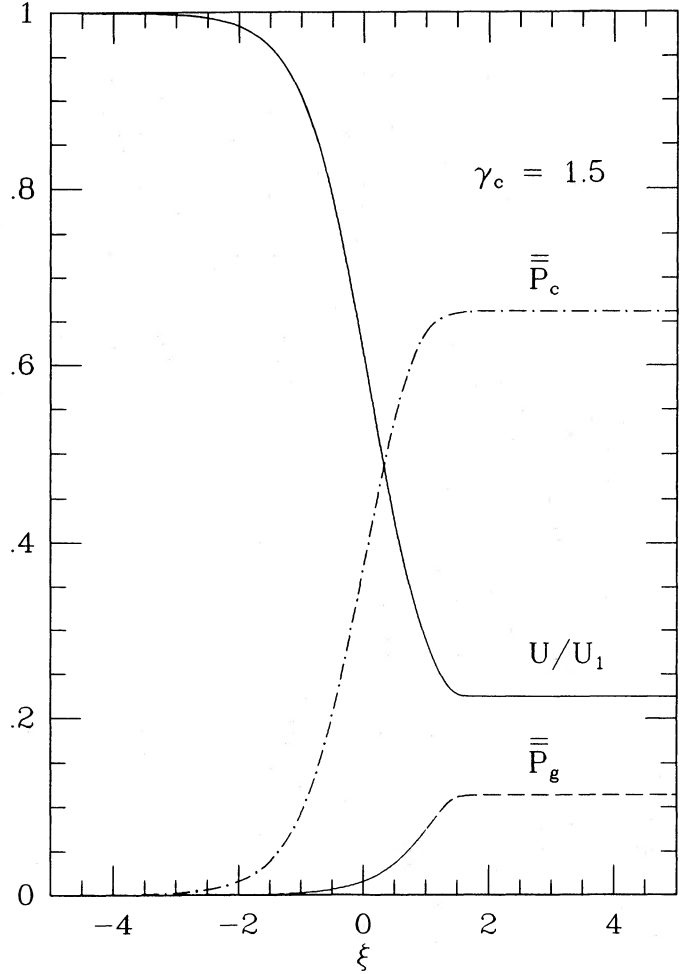


FIG. 5b

FIG. 5.—Same as Fig. 4 for the nonradiative Balmer-dominated shock

$F \leq 10^3$ (Balmer) or $F \leq 10^2$ (radiative). Notice that higher heating rates can be achieved with larger values of γ_c . Heating by compression is also important.

The accumulated dissipative heating per atom as a function of distance is

$$H(\xi) = \int_0^{\xi} \frac{h}{n} dt = \frac{\bar{\kappa}}{U_1^2 n_1} \int_0^{\xi} h d\xi, \quad (17)$$

where $H(\xi)$ is explicitly independent of the diffusion coefficient and is shown in Figures 8a–8c. For $\gamma_c = 4/3$, the dissipative energy given to an atom when the temperature is about 3.5×10^5 K, is 4.2×10^{-11} ergs for the X-ray shock (Fig. 8a) and is 2.8×10^{-11} for the nonradiative shock (Fig. 8b), while the maximum heat furnished to the gas by the former is at the shock front and is 2.0×10^{-10} ergs atom $^{-1}$.³ This was for $\gamma_c = 4/3$. However, for $\gamma_c = 1.5$ the heat dissipated into the gas in the X-ray shock reaches 3.5×10^{-11} ergs atom $^{-1}$ at a temperature of 3.5×10^5 K, compared to the maximum for the nonradiative shock (with a final temperature of 3.5×10^5 K) of 3.1×10^{-11} ergs atom $^{-1}$. From these results, we see that the dissipative heating alone provides sufficient energy to over-

³ The importance of compressive heating can be seen from the total requirement of $(3-5)kT \sim 10^{-9}$ ergs atom $^{-1}$ needed to reach 2.4×10^{-6} K.

come the 20 eV atom $^{-1}$ (3.2×10^{-11} ergs atom $^{-1}$) losses to hydrogen only after the temperature reaches about 3.5×10^5 K. Although the dominant heating derives from the compressional amplification of the dissipative portion, it is clear that cooling is not totally negligible and that self-consistent modeling would be needed for an accurate description.

We now explore the evolution of the ionization fraction in the precursor region, relaxing our previous assumption that the ionization temperature of 3.5×10^5 K for the H α shocks was necessarily the final postshock temperature. The extra equation describing the ionization fraction is

$$\frac{df}{dt} = n_e c(T)(1-f), \quad (18)$$

where $c(T)$ is the ionization coefficient of hydrogen and is tabulated in many rate tables (e.g., Edgar 1986), and $n_e = n_H f$. With a change of variable from t to ξ , we get

$$\frac{df}{d\xi} = \left[\frac{n_1 \bar{\kappa} c(T', f)}{U_1^2} \right] \frac{f(1-f)}{y^2(\xi)}. \quad (19)$$

This differential equation is integrated using the usual fourth-order Runge-Kutta method to solve both for T and f . For the

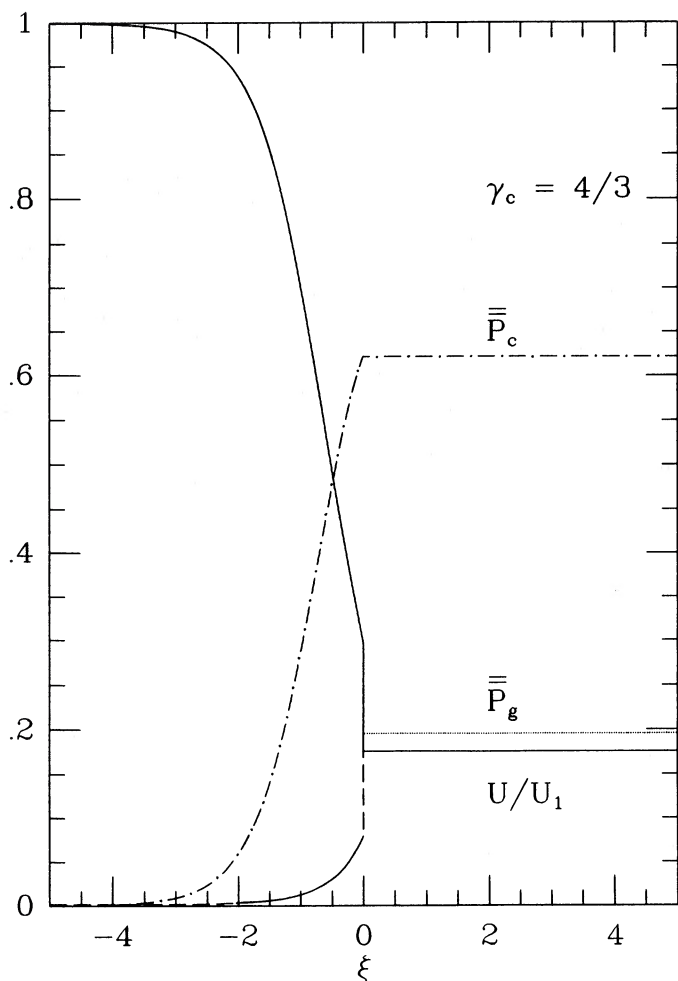


FIG. 6a

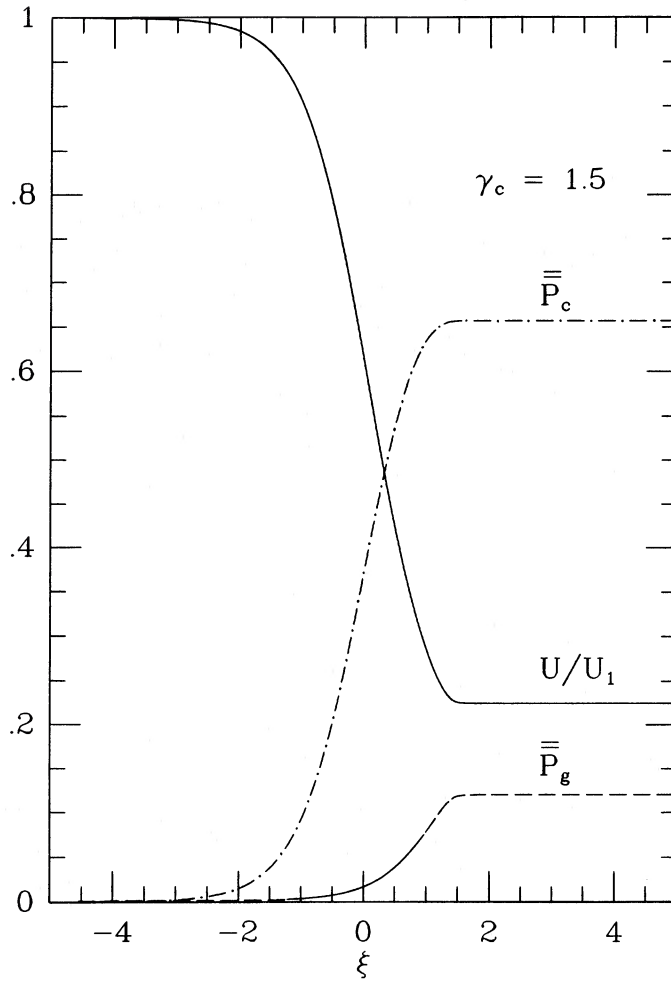


FIG. 6b

FIG. 6.—Same as Fig. 4 for the radiative shock

TABLE 2
MODEL PARAMETERS FOR THE CYGNUS LOOP

Parameter	Set Number 1 (X-Ray)	Set Number 2 (H α)	Set Number 3 (Radiative)
A. $\gamma_c = 4/3$			
Density (cm^{-3}), n_H	0.11	0.47	1.5
Shock velocity, U_1 (km s^{-1})	1110	365	230
Overall compression ratio, r_{12}	6.05	5.73	5.72
$\delta(P_{c1}/P_{g1})$	20	4.5	0.13
$\beta(8\pi P_{g1}/B^2)$	0.02	0.1	3.3
Sonic Mach number, M_{s1}	283	93	25
CR pressure, P_{c2} (cgs)	2.02×10^{-9}	8.8×10^{-10}	2.2×10^{-9}
Gas pressure, P_{g2} (cgs)	4.25×10^{-10}	2.54×10^{-10}	7×10^{-10}
BB/P_{g2}^1	7	5.5	5.1
BB/P_{c2}^1	1.45	1.6	1.6
P_{c2}/P_{g2}	4.8	3.4	3.2
B. $\gamma_c = 1.5$			
Density (cm^{-3}), n_H	0.14	0.42	1.2
Shock velocity, U_1 (km s^{-1})	1450	400	270
Overall compression ratio, r_{12}	4.71	4.44	4.45
$\delta(P_{c1}/P_{g1})$	15	5	0.16
$\beta(8\pi P_{g1}/B^2)$	0.03	0.1	2.65
Sonic Mach number, M_{s1}	370	102	21
CR pressure, P_{c2} (cgs)	4.6×10^{-9}	1.0×10^{-9}	1.3×10^{-9}
Gas pressure, P_{g2} (cgs)	4.0×10^{-10}	1.8×10^{-10}	2.3×10^{-10}
BB/P_{g2}^1	16	8.5	8.3
BB/P_{c2}^1	1.4	1.5	1.5
P_{c2}/P_{g2}	11.4	5.7	5.5

¹ $BB = \rho U_1^2 + P_{g1} + P_{c1}$.

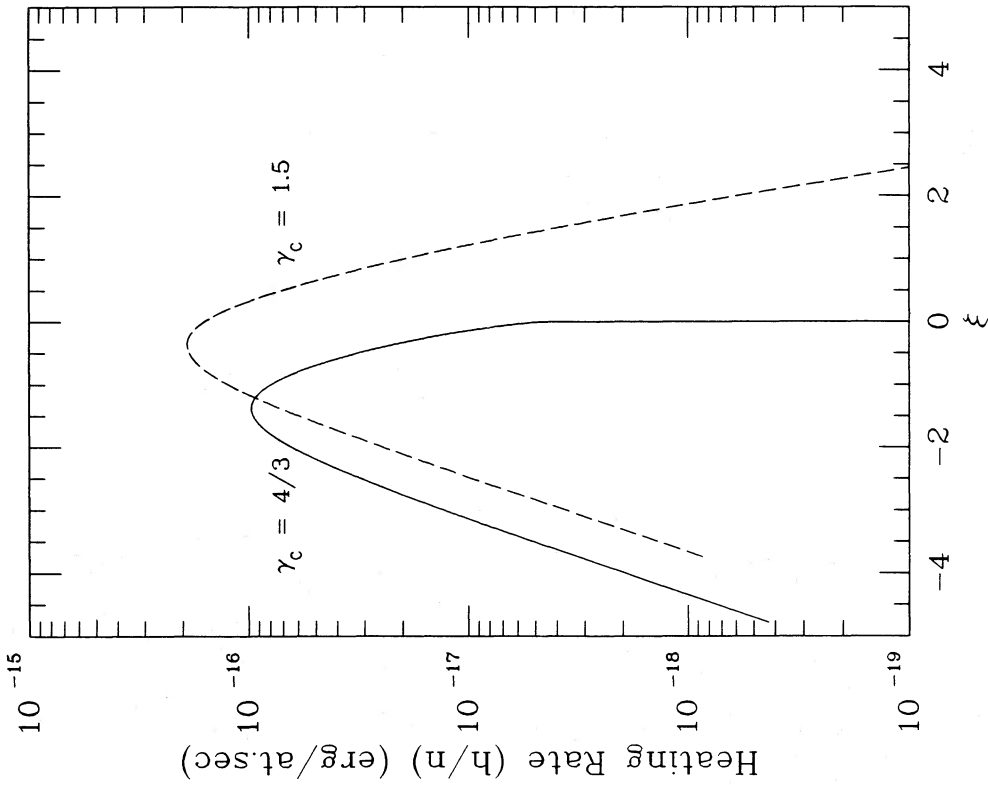


FIG. 7a

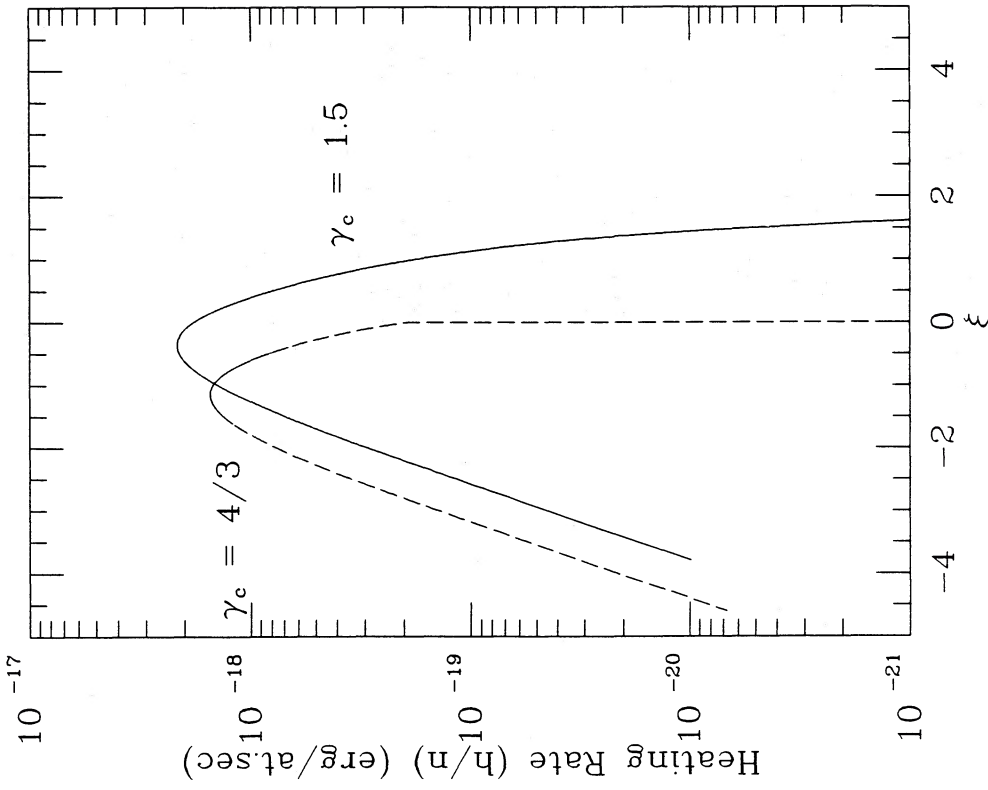


FIG. 7b

FIG. 7.—Spatial structure of the heating rate (h/n) for the three cases: (a) X-ray, (b) H α , and (c) radiative shocks

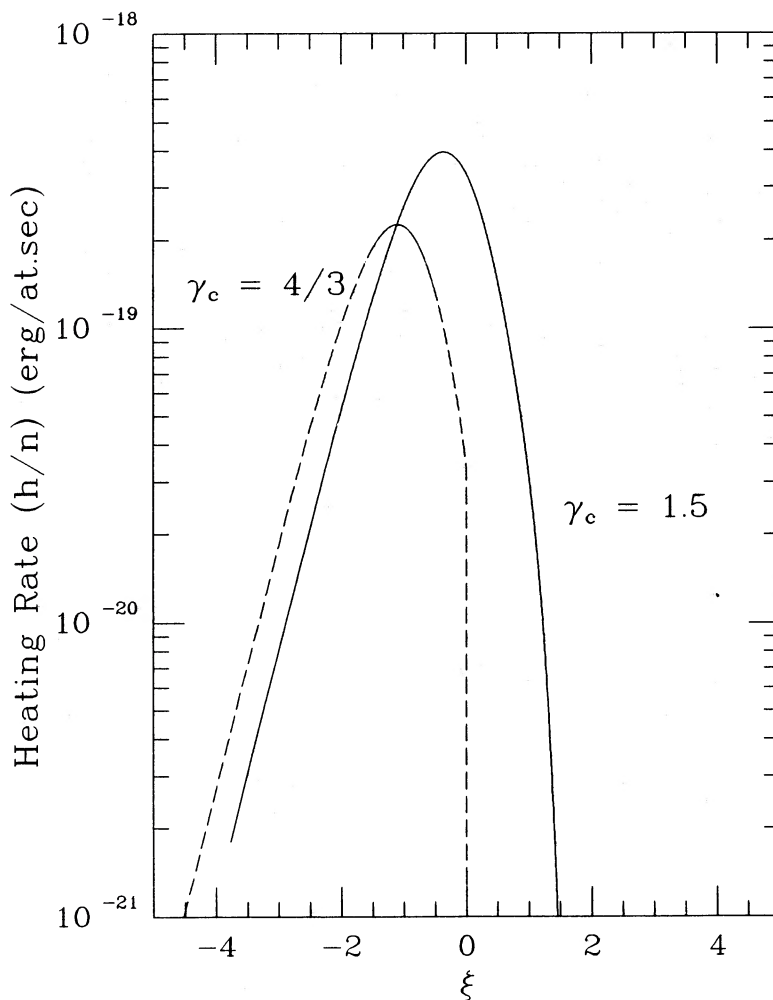


FIG. 7c

X-ray shock, the ionization fractions and the temperatures are shown in Figures 9a–9b and Figures 10a–10b, respectively, for different values of $\bar{\kappa}$. We notice that for low values of $\bar{\kappa}$ the precursor ionization is small, and it reaches 1 for $\bar{\kappa} \geq 10^{24} \text{ cm}^2 \text{ s}^{-1}$.

Let us now pursue the possibility that the H α and X-ray shocks are one and the same, a possibility noted by Raymond (1987) while discussing our results. In this scenario, the Balmer line radiation occurs at the ionization zone in the CR precursor of the shock. The Balmer line width constrains the ionization zone temperature to be $\sim 3.5 \times 10^5 \text{ K}$, while the eventual postshock temperature is $2.4 \times 10^6 \text{ K}$. The X-ray shocks in fact satisfy the flux requirement of the H α shocks perfectly ($n\nu = 0.136 \times 1110 = 151 \times 10^5 \text{ cm}^{-2} \text{ s}^{-1}$ vs. $0.467 \times 365 = 170 \times 10^5 \text{ cm}^{-2} \text{ s}^{-1}$). We see from figures 10a and 10b that having the ionization temperature of hydrogen about $3.5 \times 10^5 \text{ K}$ requires $\bar{\kappa}$ slightly greater than $10^{25} \text{ cm}^2 \text{ s}^{-1}$. We notice that the expression between square brackets in equation (19) is of order unity for the steepest increase in f (see Figs. 9a–9b). Moreover, it can be shown by using the energy equation (8) and equation (19) that for ionization at T the diffusion coefficient has the approximate value

$$\bar{\kappa} \sim \frac{2U_1^2}{n_1 C(T)}. \quad (20)$$

This expression is valid only for temperatures less than 10^5 K . Figure 11 shows the temperature at which $f = 0.6$ is achieved versus $\bar{\kappa}$. The required $\bar{\kappa}$ is $2 \times 10^{25} \text{ cm}^2 \text{ s}^{-1}$, the corresponding F is 2000 (the mean free path to the Larmor radius ratio). The corresponding characteristic length $\bar{\kappa}/U$ is $2 \times 10^{17} \text{ cm}$ and the characteristic acceleration time scale $\bar{\kappa}/4U^2$ is $5 \times 10^8 \text{ s} \sim 20 \text{ yr}$, a comfortably short time.

There is some evidence that the Cygnus Loop has an extended X-ray emission (about $\sim 10'$ beyond the bright limbs). Raymond *et al.* (1988) implied that it could derive largely from dust scattering of the X-rays. However, the present theory can be tested to see whether its predicted temperature and surface brightness structures are consistent with the observed “halo.” The joint H α –X-ray shock model required a diffusion coefficient of order $2 \times 10^{25} \text{ cm}^2 \text{ s}^{-1}$, which yields a characteristic length $\bar{\kappa}/U_1$ of about $1.5 \times 10^{17} \text{ cm}$. If we use the canonical distance of 770 pc (Minkowski 1958), and an exponential intensity decrease of less than 10^{-3} (Ku *et al.* 1984), we get roughly an angular size greater than $2'$. The diffusion coefficient may increase away from the shock giving a broader precursor which may increase the angular size of the halo. The temperature structure as a function of distance for the X-ray case is shown in Figure 12. Clearly any shock halo would have to be sandwiched between

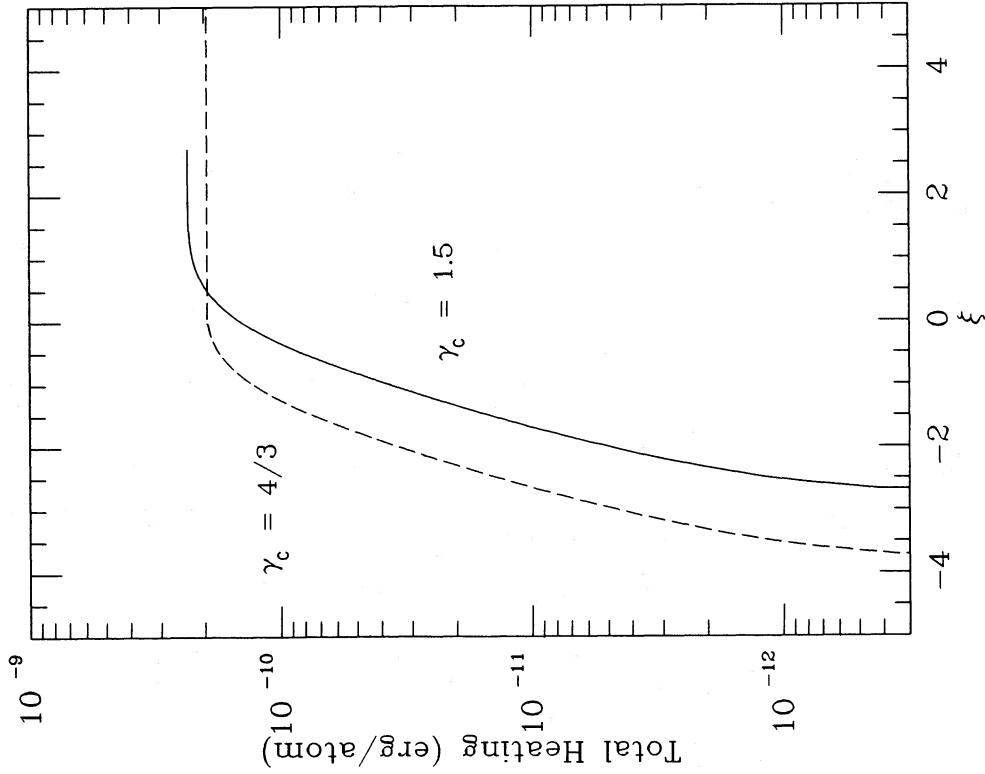


FIG. 8a

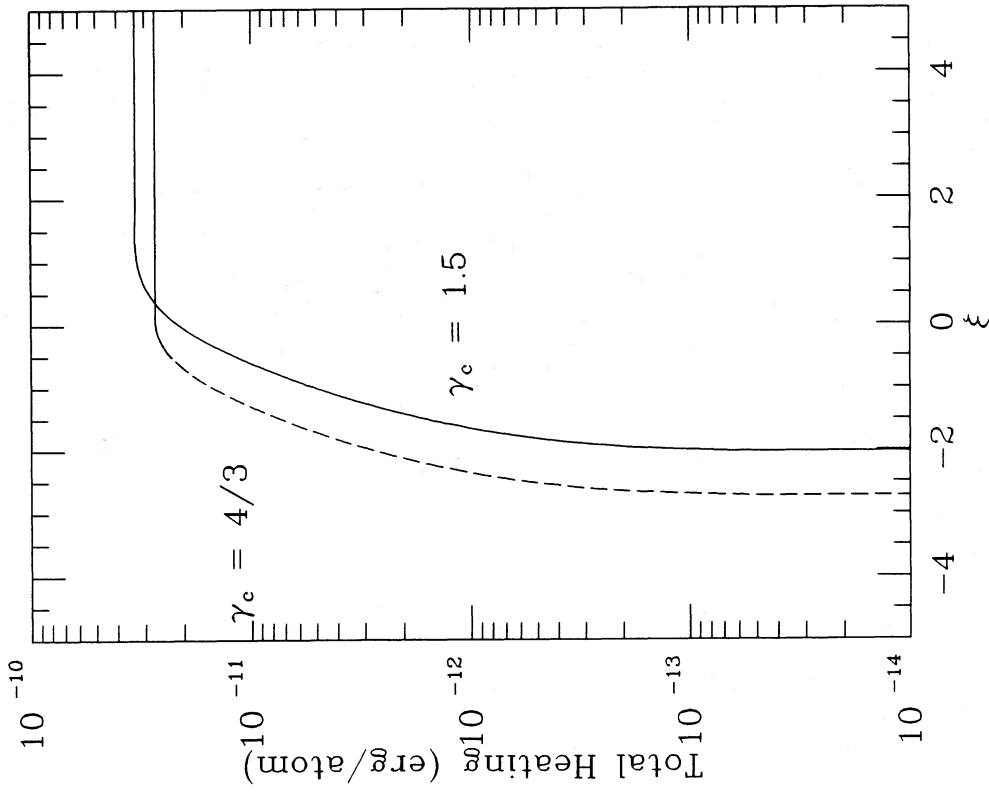


FIG. 8b

FIG. 8.—Integrated heating due to wave damping. (a) X-ray, (b) H α , and (c) radiative shocks. Compressional amplification has been ignored.

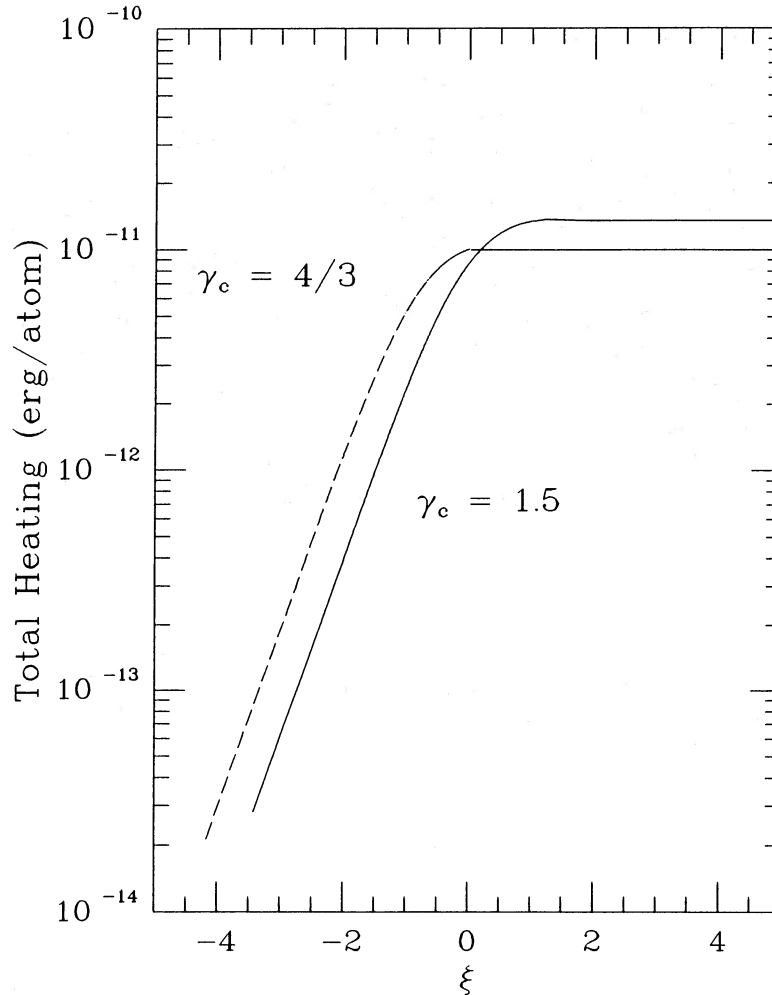


FIG. 8c

the $H\alpha$ “filament” at 3.5×10^5 K and the final 2.4×10^6 K “postshock” region.

IV. DISCUSSION AND CONCLUDING REMARKS

The three shock types known herein as X-ray, $H\alpha$ or non-radiative, and radiative have postshock temperatures and a density constraint (n_2 , $n_0 v_0$, and $n_0 v_0^2$, respectively) which can be matched either by gas pure shocks (with parameters given in Table 1) or by cosmic-ray shocks with associated wave dissipation (with parameters given in Table 2). In fact, for a particular choice of cosmic-ray diffusion coefficient, $\bar{\kappa} \approx 2 \times 10^{25}$ cm² s⁻¹, the X-ray and the $H\alpha$ shocks can be the same with the hydrogen ionization taking place in the CR precursor before the temperature rises to the final value shown in X-ray emission. This collapse to one solution is possible only because of the gradually increasing temperature in the precursor. Our solution suggests that for $\gamma_c = 4/3$ the $H\alpha$ emission in the ionization zone should be found to be about 0.1 pc ($\sim 30''$ at 770 pc) outside of the completed transition (see Fig. 17, below). Verification of this dimension would considerably strengthen the case for CR-accelerating shock presence.

There are several aspects of the Cygnus Loop shocks which have resisted explanation in the pure gas shock interpretation, yet have possibly simple significance in the present models. We have mentioned that Raymond *et al.* (1988) found that the ram

pressure for the Spur radiative shock was roughly an order of magnitude higher than the thermal pressure in the recombination zone. This is a straightforward consequence of cosmic-ray acceleration, although modeling including the radiative cooling needs to be done to learn more about the details in this case.

A second small problem is that the $H\alpha$ shocks have been found to be extremely common around the Loop edge as though they occur in the most pervasive low density. One would have expected these characteristics to belong to the X-ray shocks whose preshock density is the common intercloud value and whose velocities were twice (400 vs. 200 km s⁻¹) those of the $H\alpha$ shocks. The specific present model, in which the $H\alpha$ and X-ray shocks are the same, satisfies this intuition nicely.

A third problem has been that the $H\alpha$ shocks do not have quite the spectra predicted for the pure shock models (Raymond *et al.* 1983). The observations by Fesen and Itoh (1985) show that $H\alpha$ is accompanied by weak [S II] emission. This [S II] is common in the recombination regions of radiative shocks but should be unmeasurable in the ionizing non-radiative $H\alpha$ shocks (unless there were a large number of density inclusions of negligible scale so that there are always radiative shocks buried in the structure; but see Hester and Cox (1986) for a discussion of the unacceptability of this view).

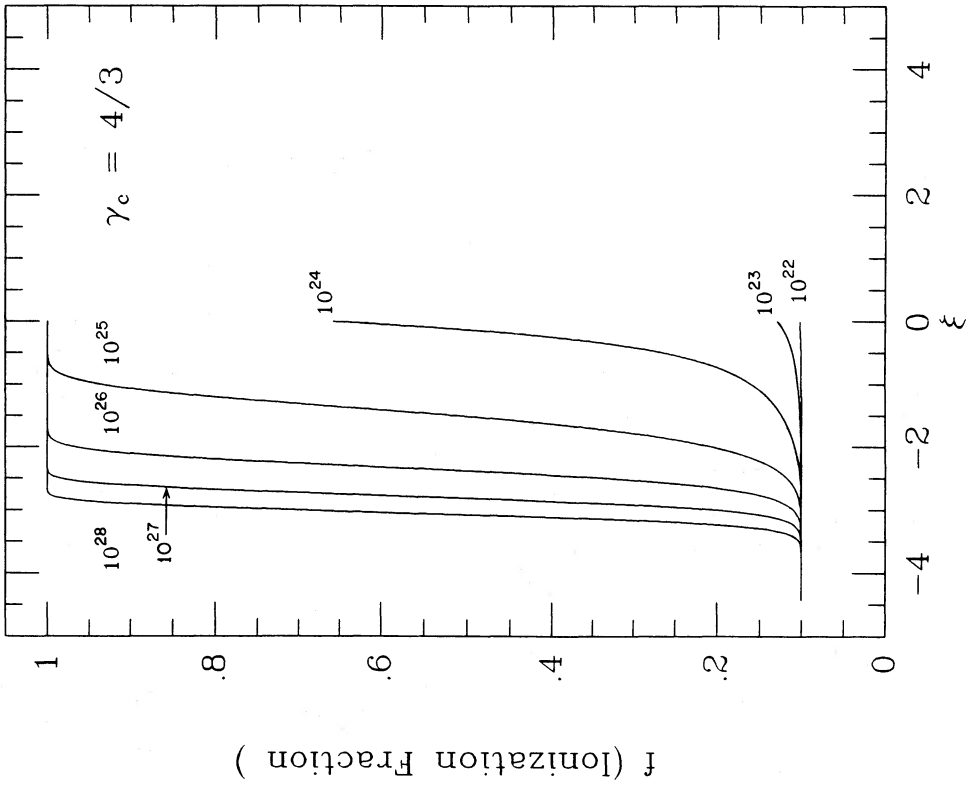


FIG. 9a

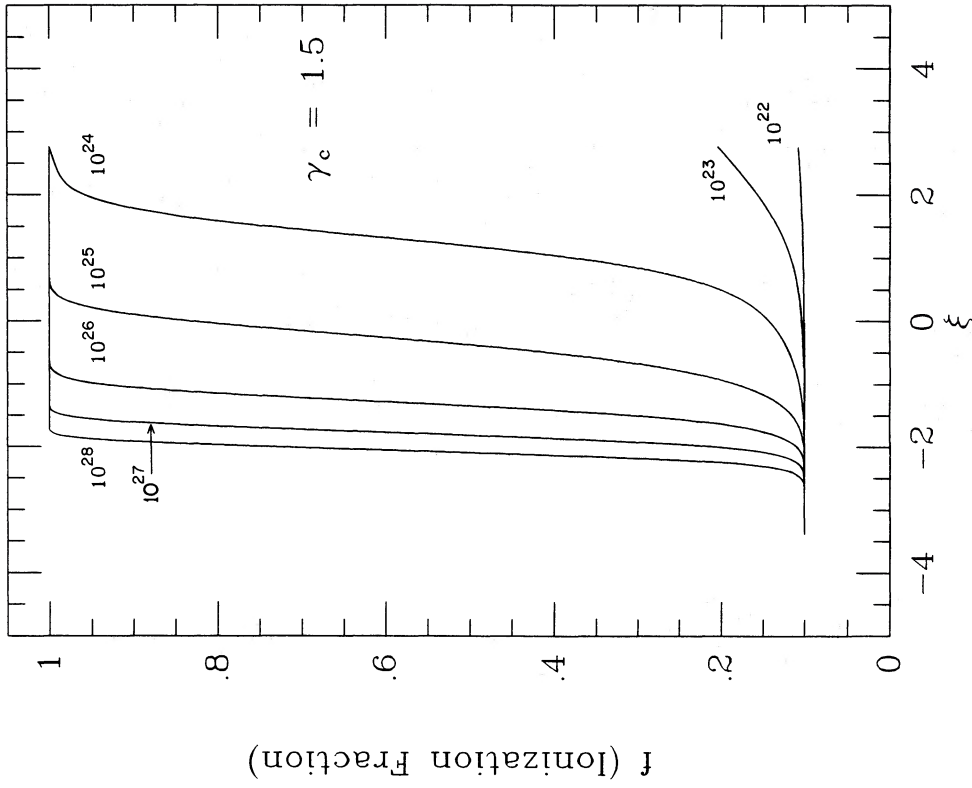


FIG. 9b

FIG. 9.—Spatial structure of the ionization fraction of hydrogen with different values of the diffusion coefficient (K) for $\gamma_c = 4/3$ (a) and $\gamma_c = 1.5$ (b). Here, f_1 was assumed to be 0.1.

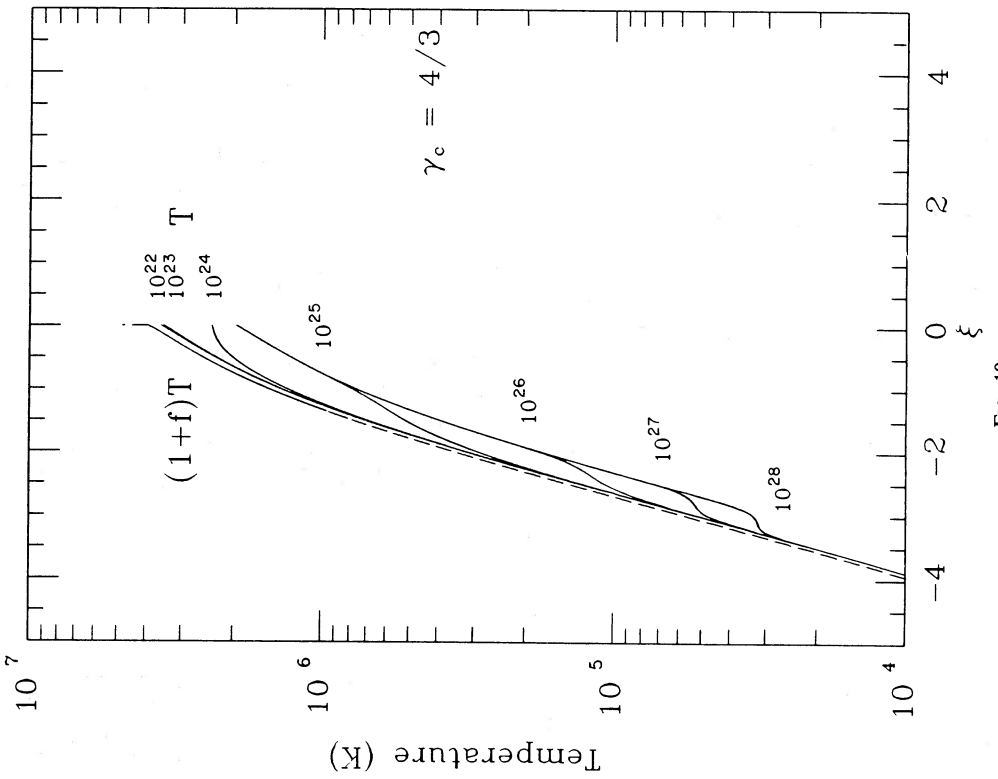
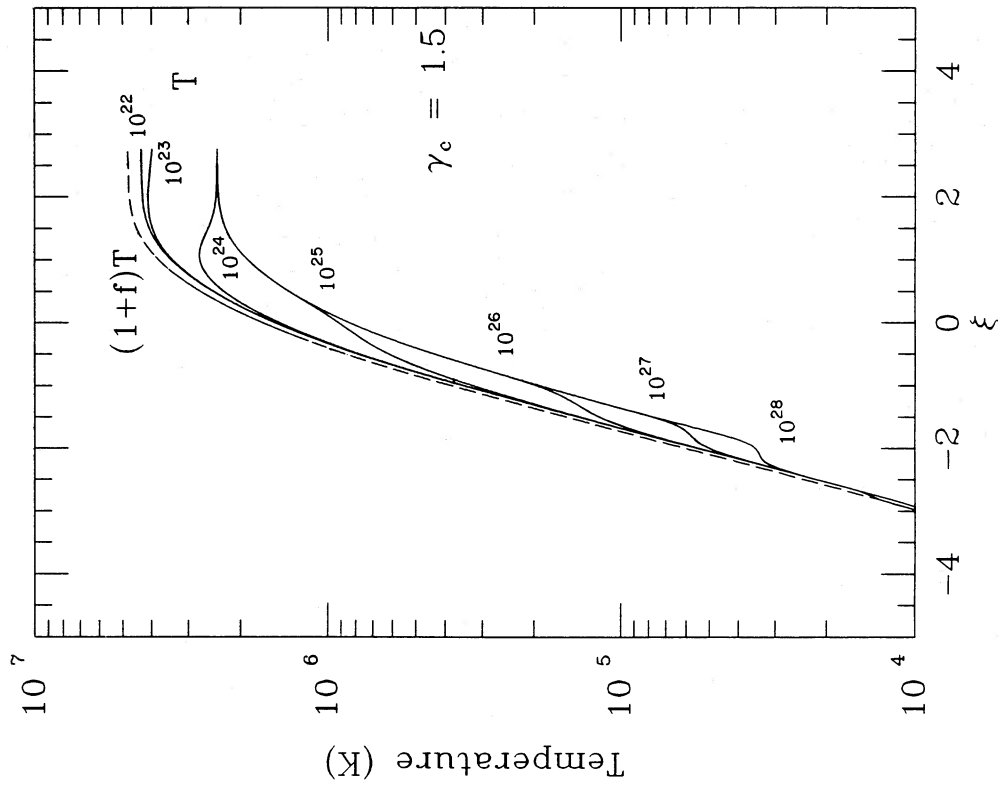


FIG. 10a

FIG. 10b

FIG. 10.—Spatial structure of the temperature for $\gamma_c = 4/3$ (a) and $\gamma_c = 1.5$ (b). Note change in transition temperature associated with ionization with the values of \bar{x} shown.

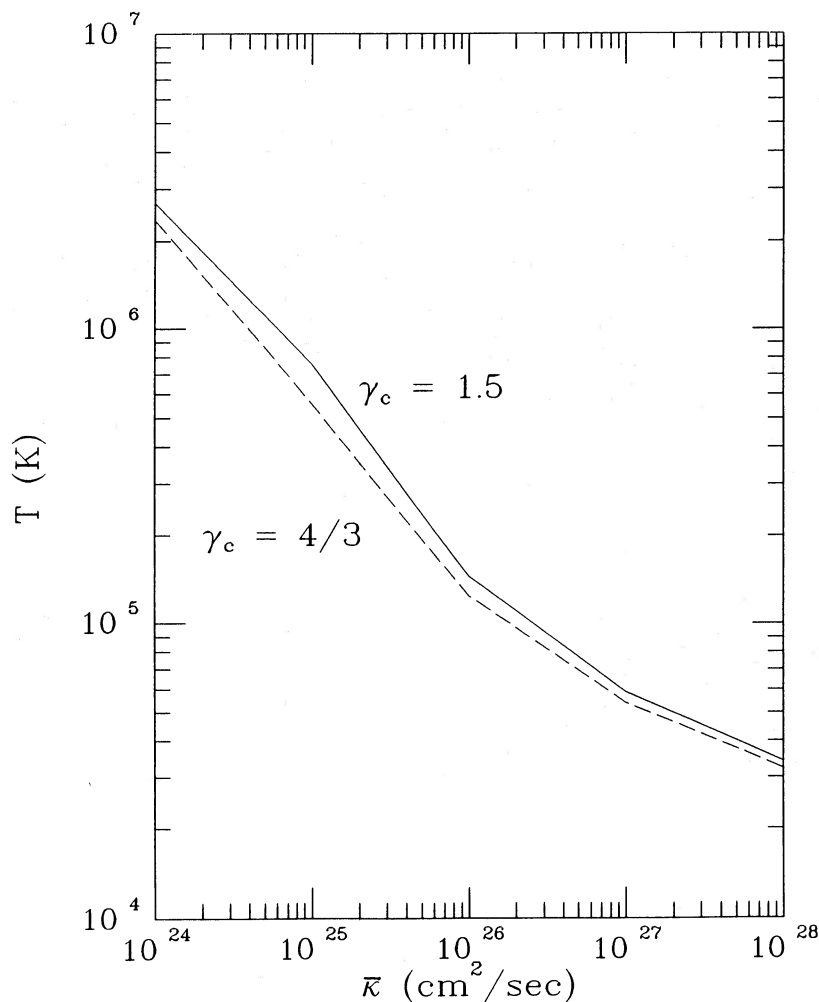


FIG. 11.—Temperature vs. the diffusion coefficient for an ionization fraction $f = 0.6$. The diffusion coefficient which corresponds to ionization at a temperature of 3.5×10^5 K is $\sim 2 \times 10^{25}$ $\text{cm}^2 \text{s}^{-1}$.

In shocks with a smoothly rising temperature in the precursor, however, an [S II] emission region is expected just outside the $\text{H}\alpha$ filament. The brightness in this region is sensitive to assumptions about preionization, CR diffusion coefficient, etc., but will warrant careful calculation if observations can confirm the relative location of [S II] and $\text{H}\alpha$. Such observations too would point very specifically toward the presence of a CR precursor and potentially measure its characteristic scale, allowing a measurement of the diffusion coefficient.

A fourth difficulty has been measurements by Kirshner and Taylor (1976) of high-radial-velocity $\text{H}\alpha$ -emitting gas over the face of the Cygnus Loop. Using these data they suggested that there was little basis for Minkowski's (1958) distance results based on his low velocities. The $\text{H}\alpha$ emission, they found, appeared to show expansion at a rate of up to 300 km s^{-1} . As a consequence, it could not be understood as arising from the $\sim 100 \text{ km s}^{-1}$ radiative shocks or the $150\text{--}200 \text{ km s}^{-1}$ non-radiative shocks (whose mass outflow velocity is only $0.75v_s$). In the standard view, it had to arise somehow from the X-ray-emitting gas (McKee, Cowie, and Ostriker 1978; Chevalier, Kirshner, and Raymond 1980; Bychkov and Lebedev 1979). (Oddly enough, the X-ray shocks should certainly be $\text{H}\alpha$ shocks as well since they ionize the incoming hydrogen, but the large line widths indicative of the high temperature have not

been found in the Balmer-dominated filaments. It could be that Kirshner and Taylor's results are telling us to look harder for filaments with the anticipated line widths.)

In our first $\text{H}\alpha$ shock model, the shock velocities of $350\text{--}400 \text{ km s}^{-1}$, and mass compression factors of $4.5\text{--}5.7$ lead to an $\text{H}\alpha$ expansion speed of $300\text{--}340 \text{ km s}^{-1}$, which is perfectly consistent with the above observations. Our radiative shocks, with velocities of about 250 km s^{-1} are also consistent with the $\text{H}\alpha$ data, but one would need to have confirmation that Kirshner and Taylor's (1976) $\text{H}\alpha$ is accompanied by the rest of the radiative shock spectrum. Finally, it may even be possible that the $\text{H}\alpha$ derives from the $1100\text{--}1500 \text{ km s}^{-1}$ composite $\text{H}\alpha$ and X-ray shocks, because the $\text{H}\alpha$ is produced in the precursor where the gas has not yet been fully accelerated. Our models predict roughly $200\text{--}250 \text{ km s}^{-1}$ for the outward velocity of the $\text{H}\alpha$ emission, also consistent with the observations.

A final possible point in favor of these models is that they show greater uniformity among ram pressures from one shock type to another than the pure gas shock results (see Raymond *et al.* 1988).

We could at this point engage in a rediscussion of the distance estimate to the Cygnus Loop, or of its energy, age, etc. We note instead only that the model ram pressure is roughly $2 \times 10^{-9} \text{ dyn cm}^{-2}$ and that the energy and age depend

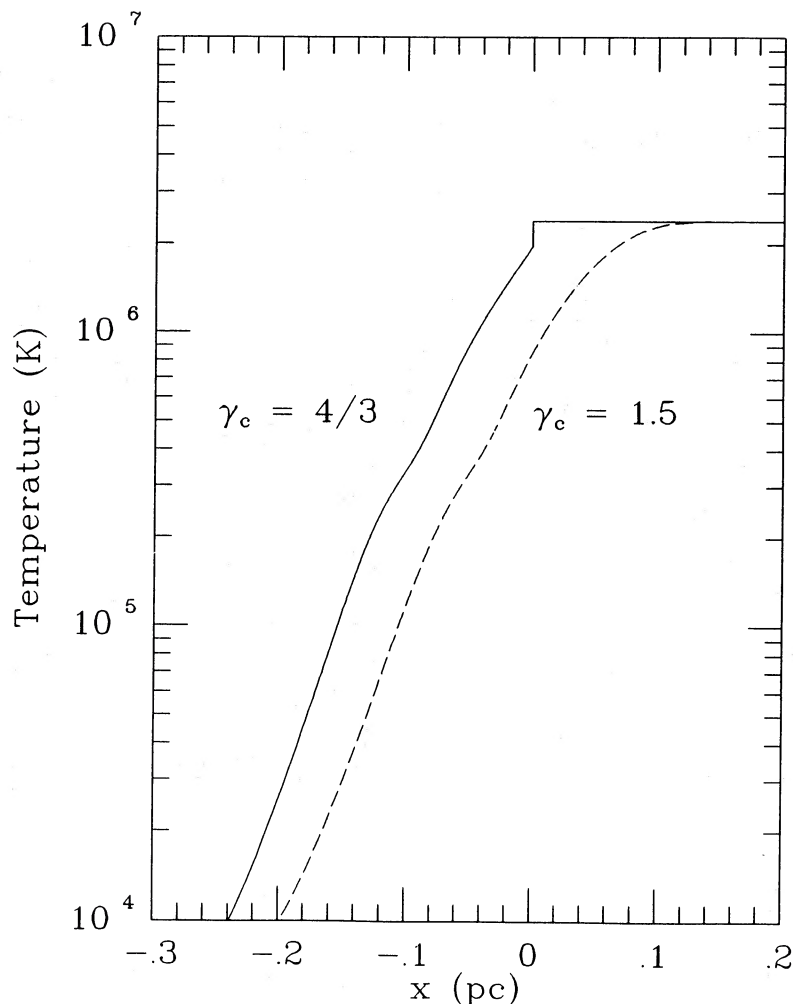


FIG. 12.—Spatial structure (x in parsecs) of the temperature for the X-ray-emitting shock

strongly on the uncertain distance. With the expansion velocity about 3 times that previously believed, the Loop would be either much younger or much farther away, and in the latter case much more energetic.

For the radiative shock, a lower density and higher velocity lead to a more extended cooling zone, one which should perhaps have already been resolved. Similarly, high $H\alpha$ expansion velocities should perhaps already have been observed in proper motions. Especially for the merged X-ray- $H\alpha$ shock, although the physical velocity of the $H\alpha$ -emitting gas is only $200\text{--}250\text{ km s}^{-1}$, as observed in the radial velocity study, the phase velocity of the expansion is the full shock velocity ($1100\text{--}1500\text{ km s}^{-1}$), and this should be seen in the proper motion. In reply to this anticipated criticism, it is our sense that our models do not apply well to the radiative shocks (see below) and that the proper motion effects have to be regarded as a measure of distance, not a constraint on shock velocity.

Our radiative shock results implied a preshock density of $1.5\text{--}1.2\text{ cm}^{-3}$, a compression factor of $4.5\text{--}5.7$ for an overall postshock density of $5.4\text{--}8.6\text{ cm}^{-3}$. The postshock thermal pressure is about 0.2 of the ram pressure. In making the model, we have supposed that it could be used for the initial shock, with the subsequent cooling done separately. If that is the case, then cooling should lead to very little further compression

since CRs dominate the pressure. Hence, the observed density of 100 cm^{-3} in the recombination zone (Raymond *et al.* 1988) cannot be attained and the model cannot work. We are quite confident, however, that CR acceleration models can be important in radiative shocks, but suggest that most of the CR pressure enhancement takes place in the cooling region as the gas and CR are further compressed. As a result, the initial shock parameters probably differ little from those of the pure gas shock (8 cm^{-3} , 100 km s^{-1}). Models encompassing this possibility do not yet exist.

In closing, we note that Cox (1987) worried that the densities found most commonly in the Cygnus Loop were in the forbidden gap (roughly $0.15\text{--}15\text{ cm}^{-3}$) of the two-phase ISM that he currently favors. He suggested that that was further evidence for SN progenitor processing of its environment. If, however, the X-ray- $H\alpha$ shock model of this paper is appropriate, then interpretation of the Cygnus Loop observations no longer requires preshock densities between about 0.11 and 8 cm^{-3} . It allows a clear segregation between cloud and intercloud densities.

This work was supported in part by the National Science Foundation under grant number AST-8643609 and by the National Aeronautic and Space Administration under grant

number NAG5-629. One of us (A. B.) was also supported by a scholarship from the Algerian Ministry of Higher Education. We thank J. Raymond for a useful discussion. One of us (A. B.)

spent two fruitful weeks at Caltech for consultation with, and advice from, Roger Blandford, Charles Kennel, and Jeff Hester, for which he is grateful.

REFERENCES

- Axford, W. I. 1981, *Proc. 17th Internat. Cosmic-Ray Conf. (Paris)*, **12**, 155.
 Axford, W. I., Leer, E., and McKenzie, J. F. 1982, *Astr. Ap.*, **111**, 317.
 Axford, W. I., Leer, E., Scadron, G. 1977, *Proc. 15th Internat. Cosmic-Ray Conf. (Plovdiv)*, **11**, 132.
 Benvenuti, P., Dopita, M. A., and D'Odorico, S. 1980, *Ap. J.*, **238**, 601.
 Blandford, R. D. 1979, *Workshop on Particle Acceleration Mechanisms in Astrophysics*, ed. J. Arons, C. E. Max, and C. F. McKee (New York: Wiley), p. 335.
 Blandford, R. D., and Eichler, D. 1987, *Phys. Rept.*, **154**, 1.
 Blandford, R. D., and Ostriker, J. P. 1978, *Ap. J. (Letters)*, **221**, L29.
 Brooks, R. D., and Pietrzyk, Z. A. 1987, *Phys. Fluids*, **30**, 3600.
 Bychkov, K. V., and Lebedev, V. S. 1979, *Astr. Ap.*, **80**, 167.
 Charles, P. A., Kahn, S. M., and McKee, C. F. 1985, *Ap. J.*, **295**, 456.
 Chevalier, R. A. 1974, *Ap. J.*, **188**, 501.
 Chevalier, R. A. 1977, *Ann. Rev. Astr. Ap.*, **15**, 175.
 Chevalier, R. A., Kirshner, R. P., and Raymond, J. C. 1980, *Ap. J.*, **235**, 186.
 Cox, D. P. 1972, *Ap. J.*, **178**, 169.
 ———. 1987, in *IAU Colloquium 101, Supernova Remnants and the Interstellar Medium*, ed. R. S. Roger and T. L. Landecker (Cambridge: Cambridge University Press), p. 73.
 Cox, D. P., and Boulares, A. 1988, in preparation.
 Cox, D. P., and Raymond, J. C. 1985, *Ap. J.*, **298**, 651.
 Courant, R., and Friedrichs, K. O. 1948, *Supersonic Flow and Shock Waves* (New York: Interscience).
 DeNoyer, L. K. 1974, *A. J.*, **79**, 1253.
 Dickel, J. R., and Willis, A. G. 1980, *Astr. Ap.*, **85**, 55.
 Dorfi, E. A. 1985, in *Cosmical Gas Dynamics*, ed. F. D. Kahn (Utrecht: Science), p. 137.
 Drury, L. O'C. 1983, *Rept. Prog. Phys.*, **46**, 973.
 Drury, L. O'C., and Völk, H. J. 1981, *Ap. J.*, **248**, 344.
 Eichler, D. 1979, *Ap. J.*, **229**, 409.
 Edgar, R. J. 1986, unpublished tables.
 Falle, S. A. E. G., and Giddings, J. R. 1987, *M.N.R.A.S.*, **225**, 399.
 Fesen, R. A., and Itoh, H. 1985, *Ap. J.*, **295**, 43.
 Ginzburg, V. L., and Syrovatskii, S. I. 1964, *The Origin of Cosmic Rays* (New York: Pergamon).
 Ginzburg, V. L., and Ptuskin, V. S. 1976, *Rev. Mod. Phys.*, **48**, 161.
 ———. 1985, *Soviet Sci. Rev. Ap. Space Phys.*, **4**, 161.
 Gronenschild, E. H. B. M. 1980, *Astr. Ap.*, **85**, 66.
 Heavens, A. F. 1984, *M.N.R.A.S.*, **210**, 813.
 Hester, J. J. 1987, *Ap. J.*, **314**, 187.
 Hester, J. J., and Cox, D. P. 1986, *Ap. J.*, **300**, 675.
 Hester, J. J., Parker, A. R., and Dufour, R. J. 1983, *Ap. J.*, **273**, 219.
 Kirshner, R. P., and Taylor, K. 1976, *Ap. J. (Letters)*, **208**, L83.
 Krysmky, G. F. 1977, *Soviet Phys. Dokl.*, **22**, 327.
 Ku, W. H. M., Kahn, S. M., Pisarski, R., and Long, K. S. 1984, *Ap. J.*, **278**, 615.
 McKee, C. F., Cowie, L. L., and Ostriker, J. P. 1978, *Ap. J. (Letters)*, **219**, L23.
 McKee, C. F., and Ostriker, J. P. 1977, *Ap. J.*, **218**, 148.
 McKenzie, J. F., and Völk, H. J. 1982, *Astr. Ap.*, **116**, 191.
 Miller, J. S. 1974, *Ap. J.*, **189**, 239.
 Minkowski, R. 1958, *Rev. Mod. Phys.*, **30**, 1048.
 Morfill, G. E., Drury, L. O'C., and Aschenbach, B. 1984, *Nature*, **311**, 358.
 Osterbrock, D. E., and Dufour, R. J. 1973, *Ap. J.*, **185**, 441.
 Parker, E. N. 1966, *Ap. J.*, **145**, 811.
 ———. 1969, *Space Sci. Rev.*, **9**, 561.
 Parker, R. A. R. 1964, *Ap. J.*, **139**, 493.
 ———. 1967, *Ap. J.*, **149**, 363.
 Pesses, M. E. 1984, *High Energy Astrophysics*, 19th Rencontre de Moriond (La Plague), ed. J. Tran Thanh Van (Gif sur Yvette: Éditions Frontières), p. 311.
 Poveda, A., and Woltjer, L. 1968, *Ap. J.*, **73**, 65.
 Raymond, J. C. 1976, Ph.D. thesis, University of Wisconsin, Madison.
 Raymond, J. C. 1979, *Ap. J. Suppl.*, **39**, 1.
 ———. 1987, private communication.
 Raymond, J. C., Blair, W. P., Fesen, R. A., and Gull, T. R. 1983, *Ap. J.*, **275**, 636.
 Raymond, J. C., Cox, D. P., and Smith, B. W. 1976, *Ap. J.*, **204**, 290.
 Raymond, J. C., Gull, T. R., and Parker, R. A. R. 1980, *Ap. J. (Letters)*, **238**, L21.
 Raymond, J. C., Hester, J. J., Cox, D. P., Blair, W. P., Fesen, R. A., and Gull, T. R. 1988, *Ap. J.*, **324**, 869.
 Scholer, M. 1985, *Proc. AGU Chapman Conf. on Collisionless Shocks in the Heliosphere: Reviews of Current Research*, ed. B. T. Tsurvtani and G. Stone (Washington, DC: AGU), p. 287.
 Shull, J. M., and McKee, C. F. 1979, *Ap. J.*, **227**, 131.
 Sofue, Y., Fujimoto, M., and Wielebinski, R. 1986, *Ann. Rev. Astr. Ap.*, **24**, 459.
 Spangler, S. R. 1985, *Ap. J.*, **299**, 122.
 Spitzer, L., Jr. 1978, *Physical Processes in the Interstellar Medium* (New York: Wiley).
 Straka, W. C. 1974, *Ap. J.*, **190**, 59.
 Straka, W. C., Dickel, J. R., Blair, W. P., and Fesen, R. A. 1986, *Ap. J.*, **306**, 266.
 Tataronis, J., and Grossmann, W. 1973, *Zs. Phys.*, **261**, 203.
 Toptygin, I. N. 1985, *Cosmic Rays in Interplanetary Magnetic Fields* (Dordrecht: Reidel).
 Troland, T. H., and Heiles, C. 1986, *Ap. J.*, **301**, 339.
 Tuohy, I. R., Nousek, J. A., and Garmire, G. P. 1979, *Ap. J. (Letters)*, **234**, L101.
 Völk, H. J., Drury, L. O'C., and McKenzie, J. F. 1984, *Astr. Ap.*, **130**, 19.
 Völk, H. J. 1984, *High Energy Astrophysics*, 19th Rencontre de Moriond (La Plague), ed. J. Tran Thanh Van (Gif sur Yvette: Éditions Frontières), p. 281.
 Völk, H. J. 1986, preprint.
 Wandel, A., Eichler, D. S., Letaw, J. R., Silberberg, R., and Tsao, C. H. 1987, *Ap. J.*, **317**, 277.
 Webber, W. R. 1987, *Astr. Ap.*, **179**, 277.
 Woltjer, L. 1972, *Ann. Rev. Astr. Ap.*, **10**, 129.
 Woosley, S. L., and Weaver, T. A. 1986, *Ann. Rev. Astr. Ap.*, **24**, 205.
 Zel'dovich, Ya. B., and Raizer, Yu. P. 1967, *Physics of Shock Waves and High Temperature Hydrodynamic Phenomena* (New York: Academic).

A. BOULARES and D. P. COX: Space Physics Laboratory, Physics Department, University of Wisconsin, 1150 University Avenue, Madison, WI 53706